A Journal of the Gesellschaft Deutscher Chemiker

Angewandte International Edition GDCh Chemie

www.angewandte.org

Accepted Article

Title: The mineral/water interface probed with nonlinear optical spectroscopy

Authors: Ellen Backus, Jan Schaefer, and Mischa Bonn

To be cited as: *Angew. Chem. Int. Ed.* 10.1002/anie.202003085

Link to VoR: https://doi.org/10.1002/anie.202003085

WILEY-VCH

10.1002/anie.202003085

The mineral/water interface probed with nonlinear optical spectroscopy

*Ellen H. G. Backus[#*1,2], Jan Schaefer[#1], and Mischa Bonn*[1]*

**corresponding authors: ellen.backus@univie.ac.at, bonn@mpip-mainz.mpg.de*

[#] *contributed equally*

1. Max Planck Institute for Polymer Research, Ackermannweg 10, 55128 Mainz, Germany

2. Department of Physical Chemistry, University of Vienna, Währinger Strasse 42, 1090 Vienna, Austria

Abstract

The interaction between minerals and water is manifold and complex: the mineral surface can be (de)protonated by water, thereby changing its charge; mineral ions dissolved into the aqueous phase screen the surface charges. Both affect the water interaction. Intrinsically molecular-level processes and interactions thus govern macroscopic phenomena such as flow-induced dissolution, wetting, and charging. This realization is increasingly prompting molecular-level studies of mineral-water interfaces. Here, we review recent developments in surface-specific nonlinear spectroscopy techniques like Sum Frequency and Second Harmonic Generation (SFG/SHG), which can provide information about the molecular arrangement of the first few layers of water molecules at the mineral surface. The results illustrate the subtleties of both chemical and physical interactions between water and the mineral and the critical role of mineral dissolution and other ions in solution for determining those interactions.

Keywords: vibrational spectroscopy, nonlinear optics, silica, alumina, calcium fluoride

10.1002/anie.202003085

TOC figure

The interaction between minerals and water is relevant for a wide range of geological, atmospheric, environmental, and electro(photo-)chemical systems. We review developments in nonlinear optical spectroscopy on a variety of mineral-water interfaces. These methods provide molecular-level details about the water organization in the direct vicinity of the interface.

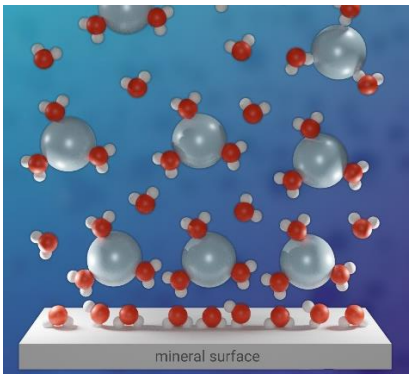

10.1002/anie.202003085

1 Introduction

Mineral/water interfaces are ubiquitous, spanning from sand in seawater to rain on rocks or window panes. Biomineralization occurs in the presence of water [1], like the formation of teeth in saliva. Also, photocatalytic reactions dissociating water into its elements can occur at the interface between certain minerals and water. Moreover, in the troposphere, water droplets nucleate on mineral particles creating mineral dust aerosols.[2] The interaction of water with minerals is also a major path for chemical reactions occurring in nature [3]. The ability of water to dissolve and precipitate minerals, thus driving their distribution on earth through rivers and oceans, is obvious. But even within the earth's crust, the role of (interfacial) water to drive geological processes has recently been emphasized.[4]

Mineral surfaces typically carry charges originating, for example, from ion substitution in the lattice when the mineral is crystallized from its melt. In contact with water, the charged state of the mineral surface could change as a result of surface reactions. For oxides, the surface charge can originate from protonation or deprotonation of groups that terminate the surface. An example of this class of molecular groups are silanols (Si-O-H) terminating the silica surface. The pH and ionic strength of the aqueous solution in contact with the surface determine the sign and degree of charging. For minerals based on ionic lattices, differences in dissolution rates of the different ionic constituents can give rise to a surface charge. One example of this is CaF_2 at acidic pH. The ready dissolution of fluoride ions compared to calcium ions gives rise to a positively charged surface. [5]

The charge at the mineral surface affects the interfacial water structure, which has consequences for the physicochemical properties of the interface and, in turn, affects mineral dissolution. This recursive interplay between the mineral surface and water, and the multitude of chemical and physical processes occurring at the interface make this system a challenge for the experimental and modeling communities alike.

The widespread relevance of the water-mineral interface has prompted many efforts aimed at obtaining a better understanding of these interfaces. Much of this work has shown that interfacial water behaves very differently than bulk water. A water molecule in the liquid bulk is, on average, tetrahedrally coordinated, donating two and accepting two hydrogen bonds. Hydrogen bonding, and the collective effects resulting from the propagating hydrogen bond network, are key in determining the properties of bulk liquid water [6]. At an interface, the hydrogen-bonded water network is interrupted, and non-tetrahedrally coordinated water molecules become more prevalent. At the macroscopic level, the termination of the bulk hydrogen-bonding network gives rise to, e.g., the anomalously high

10.1002/anie.202003085

surface tension of the free water surface and the anomalous drop in the dielectric function from ~80 in the bulk to ~3 at interfaces.[7] The complexity of aqueous interfaces is further increased by the fact that their surface is neither flat nor characterized by a uniform charge density, but is instead heterogeneous in both morphology and charge distribution.

Many continuum models exist to describe the interaction between a charged mineral surface and an electrolyte solution. The Gouy-Chapman model, based on the Poisson-Boltzmann equation, is presumably the most widespread. This mean-field description assumes, for the surface, the water, and ions dissolved in the water, respectively, that: (i) the surface is homogeneously charged, and spatially perfectly sharp, (ii) ions are point charges, interacting only via Coulomb interactions; and (iii) water is a homogeneous dielectric continuum.

None of these assumptions is rigorously valid, and their shortcomings are most apparent on short length scales. Over longer length scales, these theories are quite reliable, since electrostatic interactions are long-ranged and local details average out. It is evident, however, that molecular-level processes underlie the most important processes and properties – even apparently macroscopic ones such as wetting – occurring at mineral-water interfaces. Therefore, it is important to understand the interfacial water structure of water/mineral interfaces.

From the perspective of modeling, mineral-water interfaces pose a major challenge. Classical molecular dynamics (MD) and *ab initio* MD (AIMD) approaches work well in bulk, but an accurate description of the interaction with surfaces remains a major challenge – even using *ab initio* approaches. As such, computational studies are only slowly beginning to provide realistic molecular-level models of mineral-aqueous solution interface reactions and structures consistent with experimental results. Moreover, simulations could play an important role in peak assignments. As this review focusses on experimental work, no simulation work is explicitly discussed.

From the experimental side, substantial progress in our understanding of solid-liquid interfaces has been made using various techniques. While this review is limited to nonlinear optical probes of mineral-water interfaces, several important breakthroughs have been achieved using other techniques: atomic force microscopy, for instance, has revealed layering of water at mineral surfaces [8]; various synchrotron-based x-ray approaches, including x-ray absorption, diffraction, and x-ray photoelectron spectroscopies have been employed to shed light on the mineral surface charge, surface chemical composition, and the near-surface ion distribution, and the water organization [9]. These techniques can probe

10.1002/anie.202003085

mineral interfaces in real-space (scanning force microscopies) or *k*-space (x-ray spectroscopies) on molecular length scales, but are both potentially rather invasive. Non-invasive optical spectroscopies, and in particular vibrational spectroscopies, can, therefore, nicely complement these methods. Linear vibrational spectroscopies have molecular specificity but are not sensitive to the interface region.

Nonlinear optics typically involves the frequency conversion of optical fields by a nonlinear interaction with a material or its surface. In vibrational sum-frequency generation (SFG) spectroscopy, an infrared (IR) and a visible (VIS) pulsed laser beam are overlapped in space and time at an interface, generating photons at the sum-frequency of the two incident frequencies. A crucial selection rule for SFG is that symmetry must be broken, which intrinsically happens at the interface between two media. Moreover, when the surface is charged, that charge will align water molecules near the surface, further breaking the symmetry. Vibrational information can be obtained by tuning the IR frequency with a vibrational mode.[10] Second-harmonic generation (SHG) is a degenerate case of SFG in which only one laser beam is used, and photons at twice the frequency of the incident field are generated. While SHG, a non-resonant second-order optical process, is non-selective to particular molecular or atomic species, SFG may report on specific vibrational resonances, for example, the O-H stretch vibrations of water. This may give rise to different physical mechanisms underlying the corresponding nonlinear responses and therefore differ in their interpretation. In addition to this, both techniques can be employed in static and time-resolved manners, which allow for retrieving information on the structure and dynamics of the system, respectively. Both techniques can also be used in a scattering geometry, providing access to the surfaces of nano- and microparticles.[11] Here, we limit ourselves to experimental nonlinear optical spectroscopy on planar interfaces.

Both SHG and SFG have been used to study water/mineral interfaces, and have proven their strength in answering some of the questions raised above. In SFG, the IR frequency is typically tuned to be resonant with the OH stretching mode of water. The intensity of the signal in the O-H stretch region is a direct measure for the degree of interfacial water alignment. The sign of the nonlinear optical susceptibility reflects the absolute orientation (pointing towards or away from the surface, on average). The spectral response provides information about the hydrogen-bonding strength of interfacial water molecules. These properties make nonlinear spectroscopy a powerful tool for the study of interfacial water near mineral surfaces.[12] By using different polarization combinations for the two incident (IR and VIS) and the outgoing SFG beams, for example, ssp (s: SFG/SHG, s: VIS, p: IR) or ppp (all beams p polarized), different tensor elements of the optical susceptibility are

10.1002/anie.202003085

addressed.[13] The relative intensity of the signals acquired under different polarization combination, reports on the preferential orientation (distribution) of the molecules at the interface, after correction for Fresnel factors. However, to obtain the orientational information, an angular distribution has to be assumed. In this context, the combination of nonlinear optics with (*ab initio*) molecular dynamics simulations – which can provide such distributions – is very powerful, but outside the scope of this paper.

10.1002/anie.202003085

2. General considerations for nonlinear optical probes of the mineral/water interface

The interfacial region probed by SFG/SHG consists of those water layers that differ from the bulk structure, often referred to as the electric double layer (EDL).[12] The EDL can be loosely defined as the interfacial structure of water and counterions that appears at the charged surface of any material and consists of the near-surface Stern layer and the diffuse layer (Fig. 1). In the Gouy-Chapman-Stern description, the surface potential decays linearly in the stern layer, while it decays exponentially in the diffuse layer according to $\varphi(z) = \varphi_0 exp\left(-z/\lambda_{Debye}\right)$ with z being the distance to the surface and φ_0 the potential at z=0. Generally speaking, the electric double layer thickness can be tuned by varying the concentration of ions in the bulk liquid; the ions in solution can screen the surface charge and thereby alter the EDL by changing the decay length of the associated surface potential – known as the Debye length λ_{Debye}. The Debye length essentially determines the spatial range over which the symmetry is broken, and thereby the probing depth of SHG and SFG. Salt-dependent studies potentially provide insights into the charge distribution across the EDL and the surface potential decay associated with it. For silica, this approach has been used with both SFG[14] and SHG[15] methods.

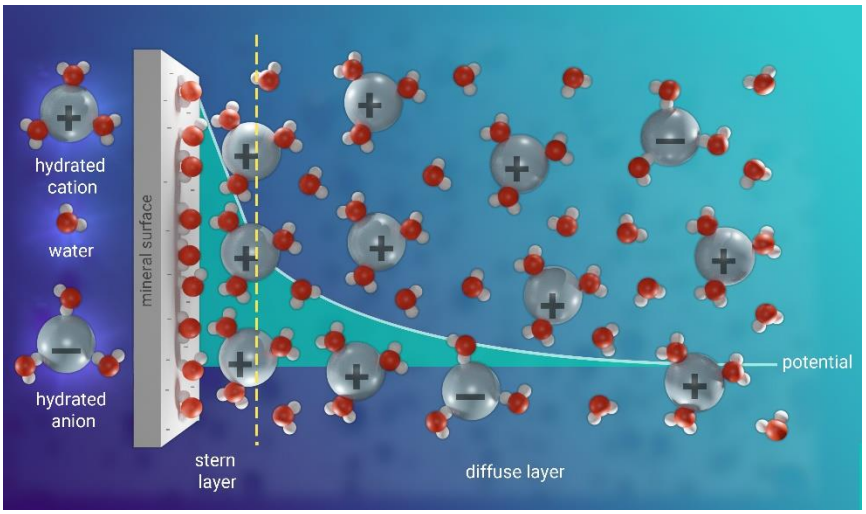

Figure 1: Schematic representation of the ion and water organization at the interface between an aqueous electrolyte solution and a negatively charged mineral surface. Also plotted is the surface potential as described by the Gouy-Chapman-Stern model.

10.1002/anie.202003085

The EDL can also be modified by changing the surface charge of a mineral in contact with water, by varying the bulk pH. In the case of silica, for example, the pH determines the fraction of deprotonated surface silanol groups. By varying the pH at fixed, rather high background electrolyte concentration (> 0.1 M), the nonlinear optical SHG/SFG response is primarily sensitive to changes in the surface-close layers which may report on the surface charge density and associated surface potential either at the surface plane (ϕ_0) or at the outer Helmholtz plane (ϕ_ζ), depending on the background electrolyte concentration. (see Refs. [14a, 16] for SHG and [16e, 17] for SFG)

It is important to note that the symmetry breaking necessary for the generation of SHG/SFG signals can have two distinct origins. Firstly, the presence of an interface, independent of its charged state, causes symmetry breaking *per se*: at the interface, the local water structure is modified due to the different H-bonding interaction with the interface than with water. If the surface is charged, the charge can cause preferential alignment of water, further breaking the symmetry. These effects can roughly be termed $\chi^{(2)}$-effects, as they affect the second-order nonlinear optical susceptibility. Secondly, the presence of a static field can give rise to a $\chi^{(3)}$-response. Simply stated, the field can polarize otherwise (bulk-like) randomly oriented water molecules, and break the symmetry in that manner, over a length scale determined by the Debye length. The magnitude of the relative contributions from the $\chi^{(2)}$ vs $\chi^{(3)}$ responses depends on the details of the system (surface charge, specific interactions between water and the surface, electrolyte concentration, etc.) and how it is probed.

Specifically, for all second-order spectroscopy techniques, the optical limit to the probing depth critically depends on the geometry of the involved beams, as it is an interplay between coherence length and Debye length.[16e, 18] Fig. 2 shows schematic pictures of the two typical geometries used in nonlinear surface spectroscopy experiments. In the evanescent wave (EW) geometry, the optical fields are enhanced in the near-surface region but decay exponentially with the decaying length $d_{evanescent}$ with distance from the surface, thereby limiting the probing depth. At high salt concentrations the debye length λ_{Debye} could be shorter than $d_{evanescent}$ in which case the λ_{Debye} determines the probing depth. In steep angle (SA) reflection geometry, the penetration depth is limited by the absorption depth of the IR beam, which, for the O-H stretch of water, results in the micrometer range. However, often the λ_{Debye} determines the probing depth of the optical signal. In the EW geometry, the evanescent wave gives rise to a penetration depth of tens of nanometers, which may be exceeded by the Debye length of the probed interface. As a result, EW-SFG is more

10.1002/anie.202003085

surface-specific than the SA analog as it preferentially reports on the signal contributions from the individual layers in the near-surface region.

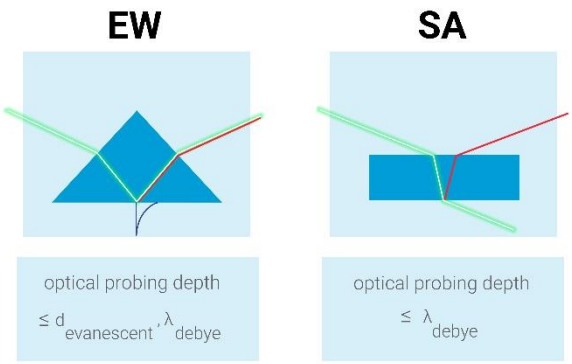

Figure 2: Schematic representation of the evanescent wave (EW) and steep angle (SA) geometry. In the EW geometry, the optical penetration depth of the incident beams is limited to the evanescent field, and the effective probing depth is determined by the smaller of the evanescent depth and the Debye length. In the SA geometry, the probing depth is only determined by the Debye length.

3 Silica

Owing to its favorable optical properties and high abundance, the silica/water interface is one of the most extensively studied buried interfaces. Silica, as a prototypical mineral can be chemically altered both in surface charge as well as the interfacial charge distribution. The surface charge of silica is tunable over a large pH range since the point of zero charge (pzc) is as low as ~pH 2.

3.1 Counterion-dependence

The pioneering work in the field of nonlinear spectroscopy of the silica/water interface was presented by Eisenthal and coworkers in 1992.[14a] In this work, they studied the silica surface in contact with lithium- and sodium-chloride solutions using SHG spectroscopy under EW geometry. They observed that independent of the cationic species, the SHG intensity decreases with increasing the ion concentration from 0.01 to 0.1 M. Since the SHG signal reflects the number of polarized and reoriented water molecules induced by the electric field, associated to the surface potential, this observation was opposite to what they expected based on the prior assumption that salt promotes silanol deprotonation and thus increases the silica surface charge. In contrast, the observed relation between ion

10.1002/anie.202003085

concentration and SHG response was rationalized with the Gouy-Chapman equation for the surface potential, which predicts a decrease of signal intensity with increasing ion concentration *c*.

An SFG study by Chou and coworkers showed a similar trend for the O-H stretch vibrational response of aqueous alkali chloride solutions in ssp polarization combination. They interpreted the results as an ion-induced perturbation of the interfacial water network.[14b] Based on the observed concentration sensitivity of the SFG signal in the order $K^+ > Li^+ > Na^+$, they concluded corresponding ion-dependent degrees of perturbation. Since this trend is not monotonic with ion size, they interpreted this observation as a combination of two counteracting effects associated with the hydration radii of the different cations: Hydration water may replace interfacial water but also promote silanol dissociation which de- and increases the SFG response, respectively. Additionally, they realized that the SFG response consists of two spectroscopic features in the H-bonded O-H stretching region (at ~3200 cm^{-1} and ~3400 cm^{-1}). Independent of the salt species, the low-frequency band appeared to be more affected by the variation of the salt concentration. Based on α-quartz/water studies at various polarization combinations,[19] Shen and co-workers argued that the low-frequency band is associated with water at (coupled) vicinal silanol groups that, when dissociated, generate a higher local surface charge density and therefore high SFG intensity. They concluded that both bands stem from the surface-close region, but the stronger concentration dependency of the low-frequency band reflects preferential ion-induced perturbance of the areas of high surface charge density.

Jena and Hore performed an SFG study under EW geometry with NaCl solutions in ssp and sps polarization combination.[14c] They found 2-3 features in the H-bonded O-H stretching region with different relative intensities for ssp and sps, respectively. They argued that with decreasing frequency, the O-H stretching band reflects more strongly H-bonded (i.e., more highly coordinated) water molecules and more symmetric over asymmetric stretching modes. In support of previous work by Chou and coworkers,[14b] they found that with increasing NaCl concentration, the overall SFG response and the ratio between low- and high-frequency bands decreases. Additionally, the sps/ssp ratio of the two main features decreases as well. In contrast to the previous interpretation,[14b] they concluded that two main species of interfacial water exist, one close to the interface with lower coordination and the other further away from the interface being more highly coordinated. They argued that the surface charge gets screened with increasing salt concentration, which results in a thinner surface layer accompanied by a relative reduction in the number of highly coordinated water further away from the surface. Based on the polarization ratios,

10.1002/anie.202003085

they additionally concluded that with increasing concentration, the average tilt angle changes from 70° to 55°, thus towards a dipole orientation more aligned with the surface normal.

In 2011, Hore and coworkers performed additional SFG experiments in ssp polarization of the silica/water system with a systematic approach in changing the ionic strength over a broad range from sub-mM up to the dissolution limit.[20] Similar to the previous results, they found an overall monotonically decreasing signal for increasing NaCl concentration. However, they were able to distinguish between four different concentration regimes, which are presented in Fig. 3a and briefly summarized below, together with the provided conclusion:

A) c < 0.5 mM: The SFG response is insensitive to the variation of the salt concentration: Ions may promote silanol deprotonation, but also screen the further distant water layers from that charge. This may give rise to a balance between an increase of the surface layer (SL) response (described by the $\chi^{(2)}$ response) and the decrease of the diffuse layer (DL) response (described by the so-called $\chi^{(3)}$ response) at this low concentration. See e.g. Refs. [14e, 16e] [21] for a more extended discussion about $\chi^{(2)}$ vs $\chi^{(3)}$ response.
B) 0.5 mM < c < 100 mM: The SFG signal decreases upon adding salt: The ions increasingly screen the surface charges which gives rise to a decreasing $\chi^{(3)}$ contribution.
C) 0.1 M < c < 1 M: A second plateau reflects the insensitivity of the SFG response towards increasing salt concentration, which is interpreted as a $\chi^{(2)}$-dominated signal with both $\chi^{(2)}$ and $\chi^{(3)}$ contributions remaining constant. In the physical model, this regime represents the transition from the Gouy-Chapman to the Stern description of the interface.
D) c > 1 M: The SFG signal continues to decrease: In this high concentration regime, the interfacial H-bonding environment gets perturbed by the ions, inducing a less ordered interfacial water structure.

10.1002/anie.202003085

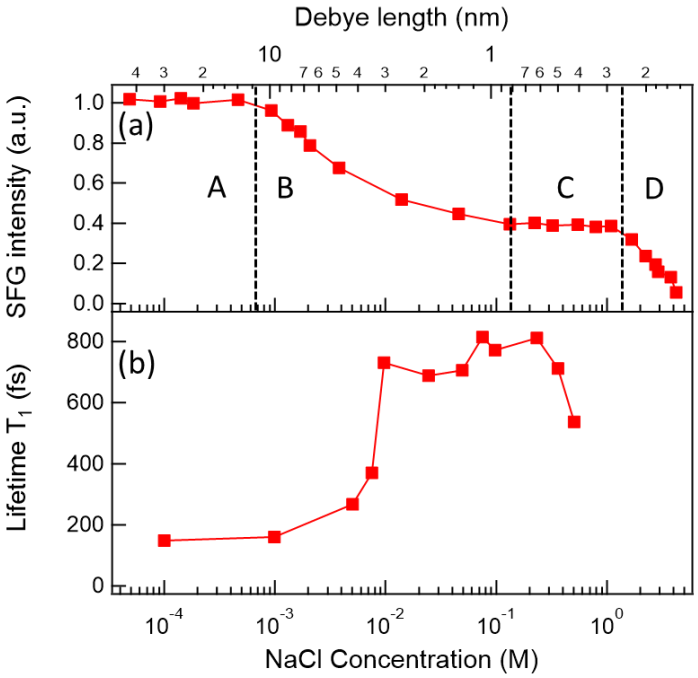

Figure 3: a) Integrated O-H stretch (ssp) SFG signal of the silica/water interface as a function of NaCl concentration. The top axis presents the theoretical Debye length, calculated based on the Gouy-Chapman model. Adapted with permission from Ref. [20]. Copyright 2011 American Chemical Society. b) Vibrational lifetimes of the O-H stretch (ssp) SFG signal of the same system, also as a function of NaCl concentration. Adapted with permission from Ref. [22]. Copyright 2011 American Chemical Society.

In complementary work, Borguet and coworkers performed a time-resolved SFG study of the same systems, also under EW geometry and in ssp polarization, which is summarized in Fig. 3b. They found that the vibrational lifetime of the H-bonded O-H stretch response at low ion concentration is comparable to that of bulk water (~200 fs) in line with the results from Hore and coworkers showing that mainly bulk is detected in SFG for low salt concentrations. In contrast, they observed substantially slower lifetimes (~700 fs) for higher ion concentrations (c >0.01 M) where the SFG response is more surface specific.[22] These lifetime measurements indicate that a salt concentration of ~10 mM is sufficient to suppress the bulk contribution. A very recent time-resolved SFG study combined with ab initio DFT-based molecular dynamics simulations revealed that ion adsorption at the silica surface can effectively change the hydrophobicity of the surface, leading to a strong reduction of the vibrational lifetime. [23]

Overall, these works highlight the role of the $\chi^{(3)}$ contribution to the nonlinear response of water at charged interfaces. It shows that for low salt concentration (c <10 mM), the (long-ranging) field-induced water response may be dominating, and the underlying structure and dynamics of those water layers behave bulk-like. On the basis of their findings, a follow-up study, as well in ssp polarization, was reported by Backus and coworkers in 2017.[14e] It

10.1002/anie.202003085

demonstrates that the SFG signal is not constant across regime A but, in contrast to regime B-D, decreases with decreasing salt concentration, which becomes evident, especially when using the SA geometry. This trend was predicted by Gonella and coworkers, who developed a model that invokes charge screening and optical interference to determine the SFG response.[16e] In an SHG study under EW geometry by Eisenthal and coworkers, a similar trend was observed, which was found to be independent of the polarization combination (p-in or s-in, all-out) or the ion size.[15] However, to achieve decent agreement between their experiments and the model mentioned above, a dramatic and exotic adjustment of the relative permittivity from 80 for bulk water to 30 for the diffuse layer was necessary. Additionally, further changes in the surface charge and / or Stern layer charge were also necessary. A follow-up study from 2019 showed that the level of the plateau at high concentration depends on both cation and anion size.[24] This was interpreted as ion-specific Stern-layer properties among the investigated alkali halides.

In 2018, Tahara and coworkers performed phase-resolved ssp measurements of the silica/water interface under high surface charge conditions (pH 12), in which they observed similar dependence on the ion concentration.[14g] Additionally, they were able to disentangle the contribution from DL and SL water species to the overall ion-dependent SFG response. As illustrated in Fig. 4a, they observed that between 10 mM and 1 M NaCl the signal decreases with ionic strength and is saturated between 2 M and 5 M. As a consequence, they considered the difference spectrum between 10 mM and 1 M to represent the DL part and the high concentration spectra as the SL part. The DL spectrum consists of two broad features at around 3200 and 3400 cm^{-1}. Since the 3200 cm^{-1} part vanished upon isotopic dilution (Fig. 4b), which is an indicator for vibrational coupling, the DL response was characterized to be bulk-like. In contrast, the SL spectrum (Fig. 4c) was insensitive to isotopic dilution, which suggested water species that are not bulk-like. Furthermore, the SL spectrum consists of two features: One pronounced positive band at 3200 cm^{-1} indicating H-up orientation with strong H-bonds to the silica surface and one weak negative one at 3500 cm^{-1} suggesting H pointing down with weak H-bonds. Based on that observation, they concluded that the topmost water layer oriented with one hydroxyl group hydrogen-bonding to the surface and the other one pointing down towards the bulk water.

10.1002/anie.202003085

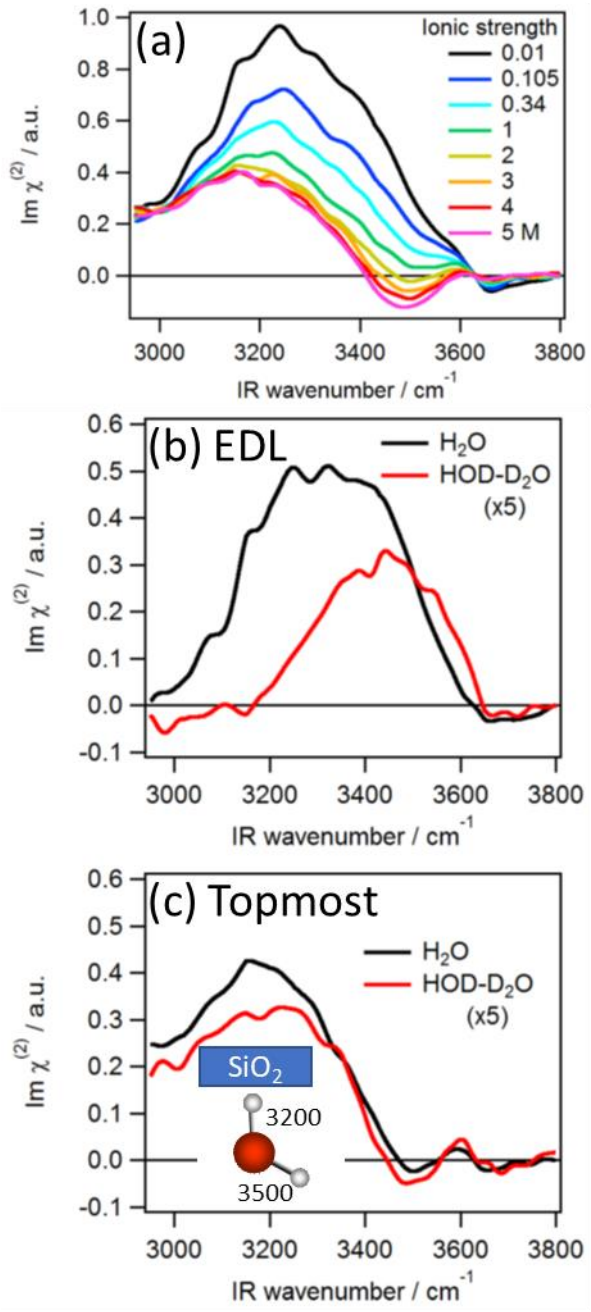

Figure 4: a) Phase-resolved SFG spectrum of silica/H_2O at pH 12 as a function of salt concentration, b) Difference spectrum between 0.01 M and 1 M for H_2O and isotopically diluted water, b) 2 M spectrum with H_2O and isotopically diluted water. HOD−D_2O means a sample with the ratio H_2O:HOD:D_2O= 1:8:16. Reprinted with permission from [14g]. Copyright 2018 American Chemical Society.

10.1002/anie.202003085

3.2 pH-dependence

The work presented by Eisenthal and coworkers in 1992 mentioned above was also the first attempt to further the understanding of the acid/base chemistry of the silica/water interface using nonlinear optical spectroscopy.[14a] By employing SHG spectroscopy under EW geometry, they recorded a surface titration curve with 0.5 M NaCl background electrolyte. As depicted in Fig. 5a, they observe a monotonic increase of the SHG response with increasing pH from 2 to 14. The titration curve consists of two turning points at pH 4.5 and 8.5 for which the authors provide a two-site silica surface model with different acidity and predominant presence of the less acidic sites (81%). The origin of the two sites is proposed to stem from different H-bonding environments of the two: The more acidic silanol species are considered to interact with water directly, i.e., pointing towards the solution. The less acidic species are thought to interact with another silanol group, i.e., lying in the surface plane. Elsewhere, these two species are also referred to as geminal and vicinal silanol groups, respectively.[16d]

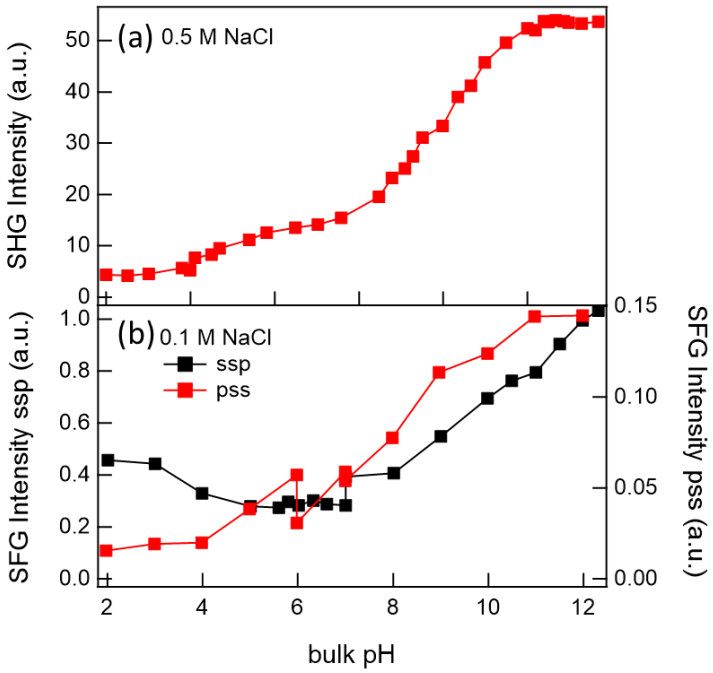

Figure 5: a) Variation of the SH electric field of the silica/water interface with changing bulk pH at constant electrolyte concentration (c(NaCl) = 0.5 M). Adapted from ref. [14a], Copyright 1991, with permission from Elsevier. b) Integrated O-H stretch ssp vs ppp polarization SFG signal (EW geometry) as a function of pH. with 100 mM background electrolyte (NaCl). Adapted with permission from Ref. [17c]. Copyright 2017 American Chemical Society.

Based on calculations of the surface potential using the Gouy-Chapman model, which assumes low electrolyte concentration, the $\chi^{(3)}$ term was deduced and used to infer

the pH dependence of the surface potential at high concentration where Gouy-Chapman is not strictly valid. The result suggested that with 0.5 M salt, the maximal surface potential for silica/water is 140 mV at pH 12.

In 2004, Shen and coworkers performed the first pH-dependent SFG study of the silica/water interface by measuring the O-H stretch vibrational response under SA geometry in ssp polarization.[19b] For all spectra, they observed two broad-band features at around 3200 cm^{-1} and 3400 cm^{-1} for more and less strongly H-bonded water, respectively. However, they realized that compared to α-quartz, the low-frequency band of fused silica appeared broader and shifted to slightly higher frequencies, suggesting that water at crystalline surfaces is more structured. After tuning the pH between 1.5 and 11 without keeping the ionic strength constant, they observed an overall monotonic increase of the SFG signal with increasing pH, which is in line with the previous SHG results by the Eisenthal group.[14a] However, they observed that the intensity of the low-frequency band varies with pH just like the SHG signal, while the high-frequency feature hardly shows any pH-sensitivity at all. In a time-resolved study by the same group, it was found that around neutral pH, the vibrational lifetime of the O-H stretching band is about 300 fs, i.e., close to that of bulk water.[25] Follow-up studies by Borguet and coworkers as well in ssp polarization demonstrated that the vibrational lifetime becomes longer with decreasing surface charge, which in case of silica/water corresponds to a decreasing pH.[26] Around pH 2, where the silica surface is neutral, and SFG is sensitive to the first few interfacial water layers, they observed lifetimes as high as 570 fs. By contrast, at high surface charge (pH 12), where the SFG probing depth is in principle limited by the Debye length of the associated surface electric field, the vibrational dynamics are faster (~255 fs) and are interpreted as bulk-like.

In 2012 the Cremer group[27] employed SFG to study the surface affinity of Hofmeister cations at the negatively charged silica surface at pH=10. Deviations from the usual Hofmeister series are observed for the Li^+ ion, explained by its strong hydration in aqueous solution.

A whole series of pH-dependent studies of silica/water was performed by the Gibbs group, starting with work from 2012,[16a] that presents pH scans with SHG under EW geometry under s-in/all-out polarization combination. In this work, they studied the impact of the cation size on the pH-dependence by using 0.5 M of 4 different alkali salts as background electrolytes. For all alkali salts, they observed a bimodal titration curve as presented by the Eisenthal group.[14a] However, the inflection point for the high pK_a species varied substantially depending on the chosen salt (from 8.3 (NaCl) to 10.8 (LiCl), which suggested that the stability of the less acidic silanol groups depends on the ion identity.

These conclusions are drawn under the assumption that the change in the SHG signal can be directly correlated with deprotonation of the interface. Also, the relative ratio of the two silanol species also seemed to depend on the salt: From the ~20/80 ratio for more/less acidic site under NaCl electrolyte that has been proposed in the Eisenthal work presented above, the relative abundance of the more acidic site can increase to 60% by using LiCl instead. Since the ion-specific surface acidity does not scale with the ionic radius but increases in the series of $Na^+ < K^+ < Cs^+ < Li^+$, they concluded that several effects contribute.

After all, cations may perturb the interfacial water structure and/or stabilize siloxide, which is why all interactions, i.e. ion-surface, ion-water, and water-surface have to be regarded:

(1) Small, hard ions such as Cs^+ interact more strongly with (i.e. stabilize) the hard siloxide.
(2) More hydration leads to more acidic sites, which holds except for Na^+.
(3) Matching water affinities can lead to shared hydration shell ion paring, which in this case means that Na^+ and siloxide match better than Li^+ and siloxide.

Subsequently, they studied the impact of different halides anions on the pH-dependence by employing the same experimental conditions.[16b] They observed that with increasing halide size:

(1) The pK_A of the more acidic silanol species shifts to lower pH, and that of the less acidic one shifts to higher pH.
(2) The titration curve gets sharper, which suggests increasing positive cooperativity between the larger (less hydrated) halides together with the cation and the surface: They concluded that large anions promote deprotonation of the more acidic species through acid-base coupling between silanol neighbors.
(3) The fraction of acidic sites increases (from 20% to 86% for sodium halides and from 45% to 91% for potassium halides), which means an increase of the surface charge at neutral pH.
(4) The effective acidity of the less acidic sites decreases, suggesting that a high surface charge makes it more difficult for the less acidic sites to deprotonate.

Additionally, they concluded that the less acidic silanol sites show negative cooperativity: deprotonation of one silanol group inhibits deprotonation of the next one.

A complementary SFG experiment [16b] interrogated the pH dependence of the O-H stretch vibrational response with 0.5 M NaI background electrolyte. Under ppp polarization combination and EW geometry, they observed an intensity increase not only from neutral to high pH but also from neutral to low pH, which differs from all the SHG results reported

10.1002/anie.202003085

about this system. They concluded that the cooperative structure between the surface, the cation and the anion that stabilizes one silanol species dissociated and the other protonated at neutral pH, displaces more interfacial water molecules than the structures formed at low or high pH which gives rise to a minimum in the SFG signal. Without providing an interpretation, they noted a ~30-40-fold decrease of the SFG response from pure water to 0.5 M NaI, much higher than reported by the Hore group for NaCl (in ssp)[20] and opposite to their own findings [16b] employing SHG which showed a 2.5-fold increase.

In another work, the same group studied the impact of salt concentration on the previously discussed cation- and anion-specific effects by comparing 0.5 M with 0.1 M solutions with SHG under s-in/all-out polarization.[16c] They observed that the cation-specific effects essentially vanish upon dilution to 0.1 M while the anion-induced changes in pH-dependence remain almost unaffected by dilution. They concluded that the alkali chlorides, except for NaCl, stabilize the less acidic silanol species in the protonated form, which stems from surface-water-electrolyte interactions. This cation-specific interfacial distribution becomes more similar for different alkali chlorides at a lower concentration. The halide-surface structure, on the other hand, seems to be so stable for the large anions that it already forms at 0.1 M.

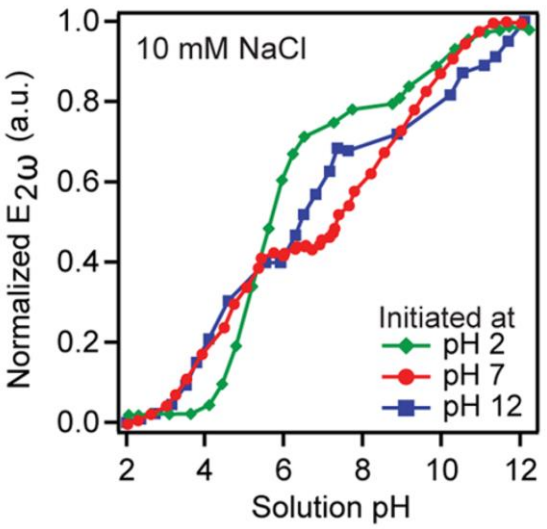

Figure 6: a) Normalized SHG intensity titration curves for an aqueous solution in contact with silica as a function of pH. The titration was started at pH 2, pH 7, or pH 12, as indicated in the legend. Adapted with permission from Ref. [16d]. Copyright 2015 American Chemical Society.

Moreover, they reported a SHG work (p-in/all-out) demonstrating that silica undergoes substantial hysteresis.[16d] As Fig. 6 illustrates by titrating from different starting pHs, they observed that the titration curve may show 2 or 3 inflection points, indicating the presence of up to 3 differently acidic silanol sites with changing relative abundance depending on the surface history. They further argued that the acidity is related to different H-bonding environments of the protonated silanol with increasing acidity in the series:

(1) Isolated (hydrophobic) species
(2) Geminal species that interact with water
(3) Vicinal species that interact with neighboring silanols

With 10 mM NaCl background electrolyte and using a p-in/all-out polarization combination, they deduced pK_a values of 3.8, 5.2 and ~9 which are all present if the starting pH was 12, while from pH 7 species (1) + (3) and from pH 2 species (2) + (3) were present. Recently, in a combined SFG and SHG work in collaboration with the Hore group[28], they showed that the SHG signal originates from the silica substrate and from the net order of water, with the substrate dominating at low pH. The SFG advantage in spectral resolution makes interpreting the SFG water signal to the net amount of ordered water difficult.

In 2013, Borguet and coworkers published on the salt sensitivity of the SFG response over the pH range of 2 to 12.[17a] Under ssp polarization combination and EW geometry, they found that upon adding 0.1 M NaCl to pure water, the SFG response changes most dramatically around neutral pH while it is mostly insensitive to the addition of salt at low and high pH: In the presence of the background salt concentration, they observed a monotonic increase of the SFG signal from pH 2 to pH 12. Without adding salt, however, they found a maximal response at around pH 8. The provided interpretation suggested that the interfacial water is most structured at neutral pH. However, in this study, the ionic strength of the pure water system was not kept constant across the investigated pH-window, which varies between 10^{-7} for neutral and 10^{-2} for pH 2 or 12. Therefore, the Debye lengths of “pure water” and 0.1 M NaCl vary dramatically around neutral pH, while becoming comparable at low and high pH.

In 2016, Chou and coworkers presented an SFG study with ssp polarization combination, using neutral pH solutions of high ionic strengths (6 and 12) of different chloride solutions, namely NaCl, LiCl, $MgCl_2$, $CaCl_2$.[14f] They found that divalent ions show a single low intensity, high-frequency water band at around ~3500 cm^{-1} suggesting that for these salts the interfacial water order is almost lost. They conclude that in contrast to alkali

10.1002/anie.202003085

ions, the local electric field of divalent ions is strong enough to polarize, reorient or displace water interacting with the surface silanol groups.

In 2016, Tahara and coworkers presented a phase-resolved SFG study (ssp polarization) on the silica/water interface under neutral (pH 7.2), acidic (pH 2.1) and basic (pH 12.1) conditions.[17b] They observed that at neutral pH and 10 mM background electrolyte, the low-frequency part of the prominent O-H stretch double feature disappears upon isotopic dilution. Therefore, they concluded that the 3200 cm^{-1} band, known to be the salt-sensitive part (in ssp), is largely caused by intra- and/or intermolecular vibrational coupling. They further noticed that the uncoupled spectrum still varies in shape and intensity with pH, owing to positive/negative contributions at high/low frequency. The low-frequency part appeared to be negative at low pH, positive at high pH, and with a negligible contribution at neutral pH. These contributions are interpreted as a convolution of 3 different water species:

(1) H-up, bonded to the siloxide
(2) H-up, bonded to the silanol oxygen
(3) H-down, bonded to the DL water

According to their interpretation, tuning the pH from basic to acidic conditions increases the number of species (2) and (3) present at the interface. They noted that in particular, the spectral component of species (3) shows a broad continuum of strong H-bonds.

In 2017, the Gibbs group published two related SFG studies on the silica/water interface. The first one compared the pH dependence of the SFG response under ssp vs. pss polarization combination, reproduced in Fig. 5b.[17c] For pss, they observed a monotonic signal increase with increasing pH, very similar to what is known from SHG studies of the same system. Based on this finding, they concluded that pss is more surface-sensitive and provides direct insight into the SL, which appears to be more ordered with increasing pH. In contrast, the SFG intensity measured using ssp experiments shows a minimum signal at neutral pH and an increase when tuning to more basic or acidic conditions. They concluded that ssp provides a larger probing depth than pss and reports on the more outer water layers that, in contrast to the topmost waters, seem to flip around neutral pH. They rationalized the findings with two possible scenarios, both being in line with the net water flip observed with phase-resolved SFG by Tahara.[17b] One scenario considers a pH-induced distortion of the SL hydration shells, the other considers the overcharging of the EDL at low pH, which usually is only expected to occur for multivalent ions.

In the second work, they tested this non-monotonic pH-dependence of the ssp SFG response with respect to the cation species of highly concentrated electrolyte solution (500 mM).[17d] At neutral pH, coinciding with the minimum of the titration curve, they observe slight differences in the signal intensity in the series $Cs^+ < K^+ < Na^+ < Li^+$, interpreted to report on the surface propensities increasing with $Li^+ < Na^+ < K^+ < Cs^+$. At low and high pH, they observed inversion of this series from which they conclude that the EDL model is only valid for a narrow range around neutral pH. For high pH, they reason that the cation adsorption is mediated by hydration water, which may result in the expulsion of Cs^+ ions but specific adsorption of hydrated Li^+. The inversion at low pH is attributed to a combination of EDL overcharging and asymmetric dehydration.

Recently, the Gibbs and Hore groups[28] made a direct comparison between pH-dependent SHG and SFG results using various polarization combinations. They conclude that the silica substrate itself can significantly contribute to the SHG signal, especially at low pH. Moreover, due to the potentially spectrally separated oppositely oriented water ensembles in SFG, care has to be taken by interpreting the SFG intensity.

3.3 The free-OH debate on Silica

Under SA-geometry, the SFG spectrum of the silica/water interface shows a broad band in the frequency region between ~3200 and 3500 cm^{-1}, commonly assigned to H-bonded OH stretching vibrations, as discussed above. However, recent work by the Tyrode group revealed the existence of an additional OH stretching band around 3680 cm^{-1}, a frequency region often referred to as the free-OH signature indicating the weak intermolecular interactions of the associated OH species. This work performed under ssp, ppp, and sps polarization, demonstrated that this high-frequency band clearly appears after special heat-treatment, for 4 hours at 1000 °C, when employing EW-geometry which amplifies the high-frequency region.[29] This sharp band at ~3680 cm^{-1} is observed, which could be the signature of the OH stretch vibration of either isolated water molecules or isolated surface silanol groups. They additionally observed that this band is the predominant one for silica/air, a nominally dry interface. However, for silica/air, the band seems to be blueshifted by ~70 cm^{-1}, compared to its silica/water analog. In addition, they performed experiments under different pH conditions, for different polarization combinations and in the presence of a positively charged surfactant (CTAB) to deduce relative signs of the

corresponding bands. Overall, they concluded that the free-OH band could be assigned to isolated silanol groups, pointing away from the surface into the water.

Another work by Backus and coworkers tested the validity of this interpretation by determining the phase information on the free-OH band directly[30] by employing phase-resolved SFG in ssp. The authors found the free-OH and H-bonded OH stretch bands being of the same sign, which indicates that the free-OH is oriented with the hydrogen pointing to the silica surface. Based on this finding, they interpreted the free-OH as a weakly interacting water species rather than an isolated silanol species. This experimental finding was rationalized with MD simulations, which identified hydrophobic patches on the nominally hydrophilic surface as a consequence of the siloxane bridges being present at the silica surface. Along with this notion, the experimentally determined increased contact angle for preheated silica was thus interpreted as an increased number of hydrophobic patches on the surface, rather than an increased number of isolated silanol groups.

3.4 Summary of silica/water

The previously reviewed studies demonstrated that the nonlinear response of silica/water is sensitive towards changes in the interfacial charge distribution. By adjusting the experimental conditions, it has thus been used as a reporter of both, the effective surface charge as well as the local concentration of ions that screen these charges. The effective surface charge can be tuned by changing the pH or, as has very recently been demonstrated by changing the temperature.[31] Moreover, the nonlinear response is also dependent on the surface preparation[29] and most likely on the type of silica as well.

The O-H stretch vibrational SFG response of water in front of a silica surface has been shown to consist of the typical double band, peaked at around 3200 and 3400 cm^{-1},[14b, 14c, 14f, 17a, 17c, 17d, 19b, 20] that is also known for bulk water[32] and the air/water interface.[33] As indicated by isotopic dilution experiments, the low-frequency part of this band is substantially affected by vibrational coupling.[14g, 17b]

Based on the concentration-dependent studies, following consistent conclusions have been drawn:

(1) In general, the nonlinear response increases with decreasing salt content of the solution,[14a, 14b, 14d, 14e, 14g, 15, 16e, 20] which can be assigned to a concentration-dependent decaying length of the surface potential, qualitatively understood with the Gouy-Chapman theory of interfaces. [14a, 14d, 14e, 14g, 15, 16e, 20] However, a recent

theoretical study claims that a good fit of SHG data with the Gouy-Chapman theory does not mean that the underlying physical situation corresponds to this model.[34] Moreover, the resulting parameters might not have physical significance.

(2) The concentration-dependence of the nonlinear response seems not only to be affected by the ion valence but also its size.[14b, 14e]

(3) At very low salt content (sub-mM), the nonlinear response has an inverse concentration-dependence, i.e., decreasing signal with further decreasing concentration. This has been assigned to optical interference, which contributes to the signal for probing depths larger than 10s of nanometers.[14e, 15, 16e]

(4) Under the EW geometry, the relative contribution of surface close-layers to the total nonlinear response is increased compared to the SA geometry. This is evidenced by comparably high signals at high ionic strength, and the impact of interference shifted to lower concentration.[14e, 15, 20]

(5) The low-frequency part of the O-H stretch SFG band is more sensitive to the variation of salt concentration and is thus preferentially resulting from the field-induced contribution $\chi^{(3)}$,[14a, 14d, 14e, 14g, 20] reporting on the more distant water layers [14d, 14e, 14g, 20], in agreement with the reported bulk $\chi^{(3)}$ for water underneath a monolayer of charged lignoceric acid.[21] At high salt concentration ($c \geq 0.1$ M), the spectral weight of the band shifts to higher frequencies, independent of the salt species, [14b, 14e] and is less affected by vibrational coupling. [14g]

The following findings are based on the pH-dependent studies:

(1) The nonlinear response of silica/water is lowest at pH 2 and increases monotonically upon increasing the pH, interpreted as a corresponding increase of the surface charge.[14a, 16a-d, 19b]

(2) Depending on the cation and anion species, the concentration and the titration direction, the titration curve shows 2 or 3 inflection points at different pH values. This is interpreted to reflect the presence and ratio of different types of surface silanol groups contributing with acidity to the overall surface charge. [14a, 16a-d] More precisely, it was concluded that there are isolated, geminal, and vicinal species with pK_a values that increase in this order.[16d]

(3) The SFG studies provided further insight and have demonstrated that the interfacial water structure is more complex than assumed based on the SHG results.[14f, 16b, 17, 19b, 35] In contrast to SHG, the pH-dependent trend of the (ssp) SFG response is not monotonic in the presence of salt but shows a minimum around neutral to slightly acidic pH.[17c, 17d, 35] This suggests a net water flip at this pH range, which was

10.1002/anie.202003085

supported by phase-resolved SFG results.[17b] Possible scenarios giving rise to this flip are a pH-induced distortion of SL hydration shells, EDL overcharging,[17c, 17d, 35] and different types of water present at the surface.[17b]

(4) The SFG response in pss polarization combination shows a monotonic trend,[17c] similar to what is observed in SHG studies with the analogical polarization combination, s-in/all-out.[16a-d] In pss polarization combination, the spectral weight of the O-H stretch response of silica/water is more on the high-frequency band compared to ssp.[17c] Together with the pH-dependent trends, it was concluded that the two polarization combinations are sensitive to different types of water, probably at different distances from the surface.[17c, 17d, 35]

10.1002/anie.202003085

4 Alumina

Another important, ubiquitous mineral whose surface charge is determined by deprotonation of surface hydroxyls is alumina, also called sapphire or corundum, which are the natural forms of alumina and contain trace amounts of impurities. This oxide serves as another good model system for studying differently charged aqueous interfaces. The difference compared to silica is, however, that these hydroxyls can be deprotonated (negatively charges), protonated (neutral) as well as over-protonated (positively charged) by tuning the pH accordingly.

4.1 pH and counterion dependence

By employing SFG under EW-geometry in ppp polarization, Pink and coworkers studied the pH-dependence of the sapphire/water interface and found a minimum in the titration curve around pH 8.[36] Changing the pH to acidic or alkaline conditions leads to an overall increase of the three-featured OH-stretch absorption band. By comparing the low and high pH spectra, they further observed substantial differences in the spectral shape. This difference was rationalized with a change in sign of individual band features, which indicates a net 180° flip of the associated water molecules. They concluded that the SFG minimum determined at pH 8 was the isoelectric point. Additionally, they demonstrated that the overall O-H stretching band scales with the number of surface hydroxyls by comparing hydrated with dehydrated sapphire surfaces.

2001, Eggleston and coworkers performed SHG measurements of the corundum/water interface under EW-geometry.[37] With background electrolyte concentration between 1 and 100 mM of different sodium salts, they studied the pH-dependence of the SHG response. In the titration curves, they found an inflection point around pH 5-6, which matched with the point of zero salt effect and was therefore interpreted as the pzc. Compared to commonly accepted pzc for alumina powders (~pH 8-9.4) and the previous SFG study without additional salt, this value was surprisingly low. Further, they found acceptable agreement between the ionic strength dependence of the SHG signal and the Gouy Chapman model for the screening of surface charge.

In 2005, Eisenthal and coworkers performed SHG experiments of the same system using the SA-geometry with p-in/p-out polarized light.[38] Adding 1 – 100 mM $NaNO_3$ of background electrolyte, they compared the pH-dependence of different faces of corundum,

namely the (0001) and $(1\bar{1}02)$ surface. They found that the pzc of single crystalline alumina is not only significantly more acidic than alumina powders, but the acidity also depends critically on the crystal face with pH_{pzc} 4.1 ± 0.4 for (0001) and pH_{pzc} 5.2 ± 0.4 for $(1\bar{1}02)$. This difference in surface acidity was assigned to differences in the coordination environment and local structure of associated hydroxyl groups.

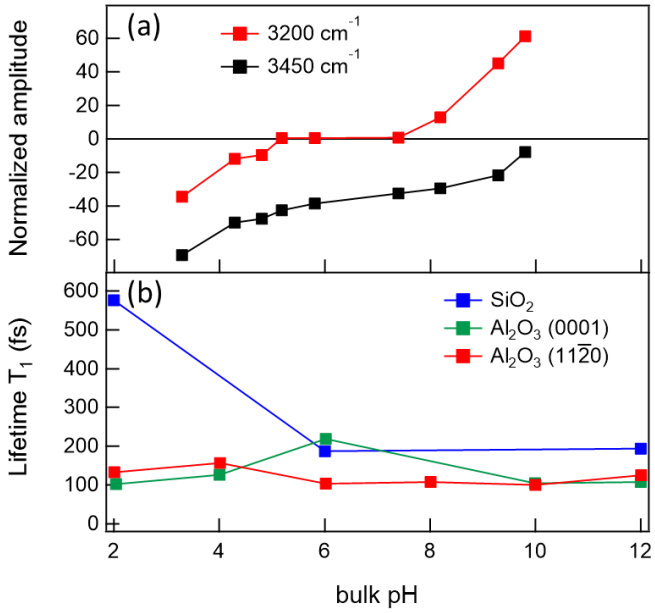

Figure 7: a) Amplitude of the 3200 and 3450 cm^{-1} signals obtained from fitting SFG intensity spectra as a function of pH. Adapted with permission from [39]. Copyright 2017 American Chemical Society. b) Vibrational lifetime of the interfacial OH species at the SiO_2/H_2O interface (blue), the Al_2O_3(0001)/H2O interface (green) and the $Al_2O_3(11\bar{2}0)$/H2O interface (red). Adapted with permission from [40]. Copyright 2017 American Chemical Society.

In 2008, Shen and coworkers reported an SFG work (in SA-geometry) on the pH-dependence of the (0001) surface and amorphous alumina,[39] with and without the addition of 0.1 M NaCl as background electrolyte and using different polarization combinations. In the spectra, they observed the typical double feature in the H-bonded O-H stretch region with signals at 3200 and 3450 cm^{-1} and an additional predominant band in the free OH region, which is in line with previous SFG work.[36] The "free-OH" band was interpreted as a reporter of the surface hydroxyl groups, for which an average tilt angle of ~26° was determined based on the polarization dependence of this band. For the H-bonded O-H stretch band, they found substantial differences in the spectral shape upon variation of the bulk pH between acidic and alkaline conditions. The results of the spectral analysis are reported in Fig. 7a showing that the 3200 cm^{-1} band flips sign around pH 6, while the 3450

cm^{-1} stays negative. Phase-resolved data confirms the flip of the net water orientation for the 3200 cm^{-1} ensemble. They concluded that the flip in water orientation reports on the surface charge upon pH variation resulting from the protonation/deprotonation state of surface hydroxyls. For alumina (0001) the pzc was determined around pH 6.3, which is again significantly lower than what is known for alumina powder or what they observed for amorphous alumina (~pH 8). This was interpreted as different forms of Al_nOH species existing on these surfaces. Additionally, they found that, if the pH is far from the pzc, the H-bonded O-H stretch band decreases substantially upon the addition of 50 mM NaCl, which was interpreted as screening of the surface charge. In the same year, another study[41] reported similar SFG spectra (ssp and ppp) and pH dependence for the corundum (001) surface, while the data were fitted with many peaks assuming many different interfacial OH species. Also in 2008, Braunschweig and coworkers[42] showed that surface disorder on a nanometer scale has a fundamental influence on the molecular structure at the (0001) interface. On an annealed surface with atomically flat terraces, they observed no SFG band in ssp above 3600 cm^{-1}. For an unannealed sample with a higher roughness, a band between 3630 and 3680 cm^{-1} appeared in line with, for example, the Shen study from 2008[39]. They conclude that this high-frequency band originates from aluminol groups in nanopores of the disordered surface. Moreover, they report a different pH dependence on the flat and rough surface, indicating that the pK value for deprotonation of aluminol groups at defect sites is different than for the atomically smooth terraces.

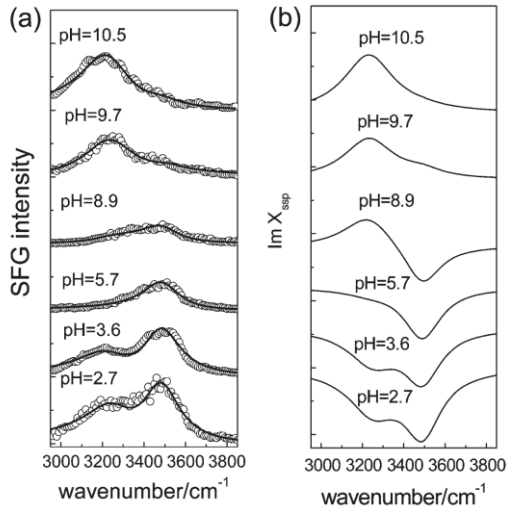

Figure 8: Intensity (a) and Im$\chi^{(2)}$ (b) spectra in the O-H stretching region for the α-Al_2O_3 ($1\bar{1}02$)/water interface at different pH values. Adapted with permission from Ref. [43]. Copyright 2011 American Chemical Society.

10.1002/anie.202003085

For the $(1\bar{1}02)$ interface in contact with water, the spectrum is different from the (0001) surface: only two bands at 3230 and 3490 cm^{-1} have been reported[43]. The lower frequency band, see Fig. 8, is assigned to interfacial water molecules, while the higher frequency band originates from the hydrogen-bonded hydroxyl groups of $AlOH_2$ on the surface. From the sign reversal of the 3230 cm^{-1} band between pH 5.7 and 7.8, the authors concluded that the pzc is ~6.7. The pK value of the deprotonation of the $AlOH_2$ is around 9.5. For the $(11\bar{2}0)$ interface in contact with water, the frequency of the dangling OH of Al_2OH has been reported to be similar to the (0001) interface.[44] A free induction decay study[45] on the (1120) surface provides indications that this free OH stretch mode might consists of two modes centered at 3644, assigned to aluminum hydroxyl groups, and 3679 cm^{-1}, attributed to a free OH stretch of interfacial water, with dephasing times of ~90 and 900 fs, respectively. The SFG response of the interfacial water molecules at ~3200 and ~3400 cm^{-1} at this $(11\bar{2}0)$ interface is sensitive to the pH with a minimum in the SFG intensity around pH 6.7.[44] The 2016 results of the Borguet group[46] are in line with these observations. However, they additionally observe a signal at ~3000 cm^{-1}, particularly clear in ppp polarization and becoming even more pronounced in the presence of ions. The authors assign this band to chemisorbed surface OH groups (i.e. aluminol groups) strongly hydrogen-bonded to the surrounding OH groups and/or to interfacial water molecules that form strong hydrogen bonds with the surface aluminol groups. IR pump-SFG probe experiments show that these OH groups undergo very fast vibrational relaxation independent of the pH of the aqueous solution, and thus the surface charge, and the ionic strength. The presence of the very strongly hydrogen-bonded species at 3000 cm^{-1} could explain the very fast vibrational relaxation. In an ambient atmosphere, only the hydroxyl signals appear in the spectrum for the $(11\bar{2}0)$ surface.[44] The Campen group showed that for the (0001) also this ~3700 cm^{-1} band appears in the ssp SFG spectrum for a hydroxylated surface in ambient air.[47]

In 2017, Borguet and coworkers presented a time-resolved ppp SFG study of alumina for different exposed crystal facets, pH conditions, and background electrolytes.[40] For the static spectra, they observed a blue-shift in the H-bonded O-H stretching band for water at Al_2O_3 (0001) compared to Al_2O_3 $(11\bar{2}0)$, which was interpreted as a comparably weak H-bonding network. In line with this conclusion, they found, as shown in Fig. 5b at pH=6 for which the surface is more or less neutral, a factor of 2 slower dynamics of that band for water at the (0001) face, compared to the $(11\bar{2}0)$ face. At charged alumina (0001) they observed faster dynamics for this band than what is known for bulk water or water at

charged silica (Fig. 7b). This was interpreted to result from (a) a fast proton transfer and/or (b) efficient coupling of the O-H stretch band with the bending overtone. In contrast to what is known for silica, they found no effect on the dynamics upon the addition of salt (0.1 M NaCl). In 2018 they showed that upon addition of 0.1 M NaF, the vibrational relaxation of water next to a positively charged alumina surface slowed down by a factor 4, suggesting that F^- alters the interfacial hydrogen bonding environment.[48] The shielding effect of the halide ions on the SFG intensity next to a positively charged alumina followed the direct and Hofmeister series with minor exceptions. At the negatively charged surface, an anion specific effect following the indirect Hofmeister series has been observed, possibly originating from ion-pair formation with the Na^+ ion. Very recently, they showed that monovalent cations have a lower binding affinity than divalent cations to the (0001) surface.[49] Moreover, the monovalent ions only attenuate the SFG signal, while the divalent ones increase the spectral intensity in the 3400 cm^{-1} region compared to neat H_2O at pH=10. Time-resolved experiments show that the cation induced restructuring of the water layer does not influence the lifetime of vibrational energy redistribution.[49]

A recent review by Lützenkirchen et al. highlights the dependence of sample preparation of the isoelectric point of sapphire.[50] As such, care has to be taken by comparing data from differently prepared samples.

5 Calcium fluoride

5.1 pH dependence

Another transparent mineral whose surface charge can be tuned by varying the pH is calcium fluoride. In 2001, Richmond and coworkers studied the pH-dependence of the O-H stretch spectrum.[51] They observed a large, broad SFG signal in ssp at low pH assigned to water strongly oriented by the positive charge of the CaF_2 generated by the dissolution of fluoride ions. Upon approaching neutral pH the signal intensity decreases due to a reduction of the surface charge. At high pH, a narrow signal at 3657 cm^{-1} has been observed originating from Ca-OH groups generated by ion exchange of F^- and OH^-. In a phase-resolved experimental and theoretical SFG work from 2016, Sulpizi and coworkers [52] showed that the O-H oscillators point with the H to the surface at low pH proving the positive surface charge proposed by Richmond and coworkers. Moreover, a comparison with

simulated spectra shows that the surface charge originates from fluoride defects rather than from proton addition to the surface as proposed as a potential mechanism for the positive charge in literature.[53] Recently, the Backus and Sulpizi group [54] showed in a joined experimental and theoretical time-resolved and 2D-SFG study (ssp), that the localized charge defects pin water molecules at the interface resulting in very fast spectral diffusion and vibrational relaxation. At high pH, the OH group was shown to point to the bulk, as expected for a Ca-OH peak. This is in clear contrast with a similar type of signal observed for the silica interface where this signal originates from water pointing to nanoscale hydrophobic patches on the SiO_2 (see section 2.3). A free induction decay ppp study by the Borguet group[55], showing timescales of 70 and 50 fs for the strong and weakly hydrogen-bonded water ensembles, revealed the presence of two oppositely oriented water populations at 3140 and 3410 cm^{-1} at neutral pH in line with a phase-resolved spectrum in Ref. [52]. For D_2O at pD 3.7, a roughly twofold slower free induction decay has been reported using ssp polarization. [56]. Moreover, they concluded that the water hydrogen bonding network is dynamically heterogeneous as different dynamics of the vibrational coherence was observed for different subensembles of H-bonded water molecules.

5.2 Counterion dependence

In a follow-up study of their early work, Richmond and coworkers studied, at a fixed positive surface charge (pH 5.8), the ionic strength dependence of the O-H stretch SFG response of the CaF_2/water interface for different salts solutions between 10^{-5} and 0.1 M.[57] Under EW-geometry, they observed that for all salts, the SFG signal decreases with increasing salt concentration, which is in line with the notion of surface charge screening in Gouy-Chapman theory. However, they found that the signal is more sensitive to the addition of SO_4^{2-} and F^- salts than to Cl^- and Br^- salts. They concluded that sulfate and fluoride screen the surface charge more efficiently than chloride and bromide. Also, they observed substantial spectral deviation from the pure water spectrum in case of fluoride, which they interpreted as additional disruption of the interfacial water structure.

In 2014, Bonn and coworkers published a work where they studied the impact of flow on the SFG spectra of water at the CaF_2 surface.[5] Under EW-geometry and ssp polarization combination, they compared flowing and resting water at different pHs. Under resting conditions, the highest response was observed at low pH, which was assigned to the interfacial order imposed by the positively charged surface as a consequence of preferential

10.1002/anie.202003085

F^- dissolution. Around pH 8, a minimum SFG signal was observed, followed by an increase towards alkaline conditions, which was interpreted as the result of dissolved carbonate replacing surface fluoride, which makes the surface more negative. Upon flow, as illustrated in Fig. 9, they observed an increase of the signal at low pH and a decrease at high pH. At pH 9.5, flow merely changes the absolute intensity but alters the spectral shape, which indicates a change in sign of the band and a net flip of interfacial water molecules. This was interpreted as a flow-induced modification of the surface charge, which, compared to static conditions, requires a change in pH up to 2 units. Similar flow-dependent changes at low pH are observed with SHG in p-in/p-out and p- and s-in/s-out polarization.[58]

10.1002/anie.202003085

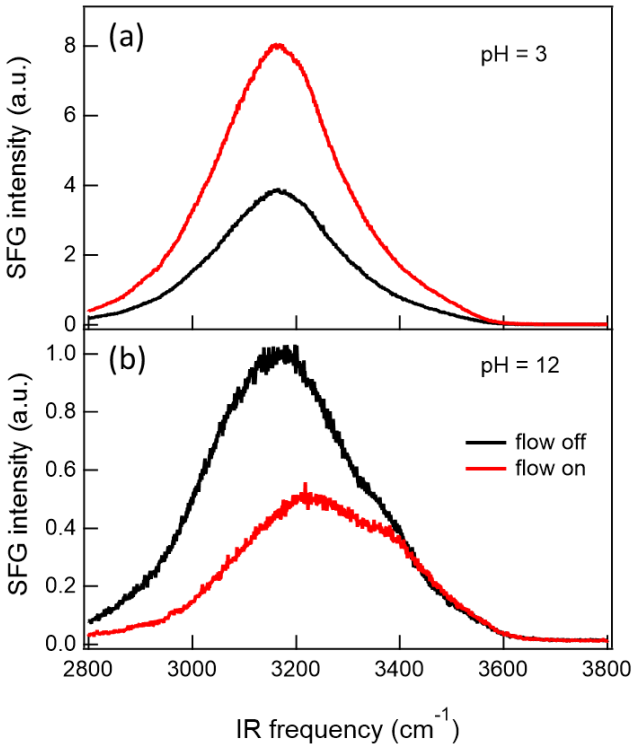

Figure 9: SFG spectrum (not normalized for the spectral envelope of the IR pulse) of the OH stretch region of the CaF_2-water interface at (a) pH 3 and (b) pH 12 under static (black) and flow (red) condition. From Ref. [5]. Adapted with permission from AAAS.

10.1002/anie.202003085

6 Titanium dioxide

The interaction of TiO_2 surfaces with water is of great interest owing to their photocatalytic activity. One of the first nonlinear spectroscopic studies of this interface was presented by Cremer and coworkers in 2004.[59] With 30 mM of different background electrolytes, they investigated the pH-dependence of the OH stretch SFG (ssp) response at thin films of TiO_2 (0.9 - 3.9 nm) on a silica substrate. Upon addition of NaCl, they found a minimum of the double-featured band at around pH 4 – 6, which matched with the isoelectric point commonly known for this system. Above and below that pH range, they observed an increase of the low-frequency feature (~3200 cm^{-1}) relative to the high-frequency one (~3400 cm^{-1}). Adding PBS (phosphate-buffered saline) buffer instead of NaCl shifted the minimum to pH 2, which was interpreted as a shifted isoelectric point due to strong adsorption of phosphate to the TiO_2 surface, similar to what they observed for silica. In the same year, Nihonyanagi and coworkers studied the adsorption behavior of water from the vapor phase on TiO_2 with and without UV pre-treatment of the TiO_2 surface.[60] Under EW-geometry and ppp polarization combination, they found that UV irradiation of the surface increases the overall H-bonded OH stretch response as well as a third feature in the free-OH stretching region. They concluded that UV irradiation leads to more ordered water on the surface as a result of increased hydrophilicity of TiO_2. In 2012 the Cremer group published a follow-up study determining the effects of cations on the interfacial water structure at the negatively charged surface.[27] It was observed that the cations followed in principle the Hofmeister series with a few exceptions potentially due to electronic properties, charge density, and hydrogen bonding ability.

In 2017, Backus and coworkers presented an ssp SFG study of water at UV-irradiated thin films of anatase TiO_2 (1 μm, consisting of 50 – 200 nm globular particles) deposited on a CaF_2 substrate.[61] They found that the two bands of the H-bonded OH stretch response have an opposite sign, which indicates two sub-ensembles of OH groups at the surface. The high-frequency band was interpreted to represent weakly H-bonded, chemisorbed OH groups at the surface that point towards the bulk water. The low-frequency band, indicating strong H-bonding, was interpreted as physisorbed water that interacts with the chemisorbed species by pointing towards the surface. The superhydrophilicity of the UV-irradiated

10.1002/anie.202003085

surface was assigned to the strong interaction between the chemisorbed and physisorbed water species. Additionally, they observed significant changes of the double-band shape upon isotopic dilution, which was assigned to vibrational coupling. In a different work, they studied the pD-dependence of the OD-stretch SFG response at 85 and 150 nm thin amorphous films of TiO_2, depicted for the 150 nm thick film in Fig. 10[62] They observed a minimum in the titration curve at around pD 5 which originates from a change of sign of the main band at around 2300 cm^{-1} when the pD crosses the pzc. This main band originates from water in the first two water layers. Additionally, high- and low-frequency bands are observed, not changing sign as a function of pD and assigned to TiOD groups and D_2O molecules directly H-bonding with the surface, respectively.

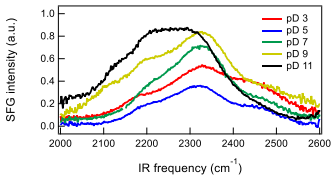

Figure 10: SFG intensity spectra in the O-D stretch region of the TiO_2-D_2O interface at different pH for a TiO_2 layer thickness of 150 nm. From Ref. [62] – Published by the PCCP Owner Societies.

7 Mica

Since mica is one of the most abundant minerals on earth, it has also been increasingly gained attention, especially for its interactions with water. In 1998, Salmeron and coworkers presented the first SFG study of the mica/water interface, using ssp polarization, investigating the adsorption behavior of D_2O depending on the humidity.[63] They observed that with increasing humidity, the typical double-band appears in the D-bonded OD-stretching region, with the low-frequency feature becoming the predominant signal. They concluded that, as the humidity increases, the sub-monolayer water structure evolves into a more ordered D-bonding network and clear absence of the free OD peak at full monolayer coverage. Another SFG study employing the SA-geometry demonstrated an azimuthal angle dependence of the OH-stretch response at mica (001), which indicated the mica

crystal structure imposes anisotropy on the interfacial water response.[64] As discussed in more detail below, several groups [65] have studied the mica-water interface in the context of ice nucleation, concluding that the surface-induced ordering of water plays an important role in the water freezing process.

8 Outlook

8.1 Experimental challenges

As mentioned before, nonlinear spectroscopy is not only surface-sensitive but also EDL-selective due to its symmetry selection rules. Intrinsically, nonlinear spectroscopy provides information about all the non-bulk-like interfacial water layers which lack centro-symmetry. Therefore, it reports not only on the surface charge but also on the distribution of the countercharges that screen the surface and form the EDL. In other words, the degree to which each individual water layer contributes to the NL signal is primarily determined by the decay of the potential associated with the surface charge. However, this convolution of signal contributions from surface-close ($\chi^{(2)}$) and distant water layers ($\chi^{(3)}$) makes the analysis complicated, as has been discussed in this review since any change in the EDL will affect the overall nonlinear response. For that reason, the experimental conditions of both, the interface and the optical setup are crucial for interpreting the results and meaningfully comparing different studies.

A recurrent issue in many studies of second-order nonlinear spectroscopy of water at charged interfaces is the fact that symmetry breaking may result not only from the reorientation but also from the polarization of interfacial water molecules. So far, it has not been possible to disentangle the two contributions to the NL signal properly. Only water species that differ in H-bonding strength and/or net orientation can be discriminated using SFG (e.g., ref. [14a, 14c, 17c, 19b]) and phase-resolved SFG (e.g., ref. [14g, 17b, 19b]). However, the H-bonded OH stretch response is a broad multi-featured band that may still hide chemically similar sub-ensembles of polarized and/or reoriented water species. Although phase-resolved SFG is evidentially a powerful tool, we caution the reader about overinterpreting low-intensity phase-resolved spectral features as this can easily lead to misleading conclusions. A good example is the assignment of the low-frequency part of the OH stretch response in the water/air spectrum which has been the subject of intense discussion,[66] and seems to be a normalization artifact.[67] Even if artifacts can be excluded, the band shape might not only report on the distributions of water ensembles under different chemical

environments but can also be affected by vibrational coupling as demonstrated for silica/water as well.[14g, 17b] If this is the case, isotopically diluted water can be used to suppress the coupling effects and to read off the "absolute" band shapes.

Another experimental option is to measure the NL response in an off-resonant fashion by employing SHG. It has been argued that this method provides a more direct relation to the surface charge as the signal seems to be less affected by orientational effects.[17d] However, it is still unclear how SHG then reflects the balance between reoriented and polarized layers if not in an additive fashion. Additionally, the chemical selectivity of the NL response is lost in SHG, and it is not clearly known how the SHG signal depends on the probing wavelength. All of this should be taken into account when comparing SHG with SFG studies and SHG studies with one another.

Moreover, for both methods, SFG and SHG, the employed beam geometry is also important for interpreting the NL signal. Since the variation in beam angles is known to alter the local field at the interface, it may affect both, the shape and absolute intensity of the spectrum. A recent work about the TiO_2/water interface serves as a good example of this problem.[62] In principle, this effect can be corrected for by invoking Fresnel factors,[68] but this requires accurate determination of refractive indices of the involved media and is therefore rarely done on these systems. An often-used geometric trick to amplify the NL response is to tune the incident beam angles to total internal reflection, which generates an evanescent field at the interface. This is especially beneficial for kinetic experiments, as it allows one to reduce the accumulation time by roughly a factor 100.[5, 69] On the other hand, EW-geometry makes the NL response more surface-sensitive, which distorts the signal contributions from surface-close and distant layers in favor of the closer ones. [18] Depending on the interfacial charge distribution, this might even lead to loss of the EDL selectivity if the Debye length exceeds the EW.

The minerals that can be studied with NL spectroscopy have to be transparent in the frequency ranges of all involved beams. For high absorptive materials, thin films deposited on a transparent material could be used. The preparation of well-defined thin films is experimentally challenging, and the measurement can be affected by multiple reflections, fluorescence, or other unknown contribution to the non-resonant background.[62] But even for the most extensively studied interface, silica/water, there is not a unifying picture for the nature of the EDL. Historically, Stern (SL) and Diffuse Layer (DL) have been approached separately through (a) pH titration with high electrolyte background concentration and (b) tuning the ionic strength around neutral pH. While (a) is sensitive to changes in the surface charge, (b) primarily reports on the Debye length by going to even sub-mM concentration.

In this context, the pre-treatment of the surface with respect to both, pH and ionic strength, is crucial for determining its current state, since silica seems to undergo massive hysteresis along with pH titration[16d] and ion exposure[15]. Besides that, there are a few caveats coming with the above-mentioned approaches:

1. At high salt concentration, the dissolved ions themselves may affect the surface charge by promoting protonation or deprotonation. Hence, the surface potential and the zeta potential are related to one another and cannot be treated separately.
2. Although the Gouy Chapman model has shown to provide a good qualitative prediction for the ionic strength dependence of the NL response,[14e] it does not yield a satisfying description over the entire concentration range. For the model to work, dramatic changes in the screening properties need to be invoked by e.g. changes in the interfacial dielectric permittivity[15, 24]. This implies that some information is contained in the NL response that has so far not been considered. Therefore, we caution the reader about relying on quantitative arguments made from GC-based model descriptions of these types of SFG and SHG experiments.

In addition, strong indications exist that SHG and SFG report differently on the nature of EDLs (e.g. Ref. [16a] vs. Ref. [17d] and Refs. [15, 24] vs Ref [14e]). Primarily, this difference is ascribed to orientational effects, which are assumed to add up differently in SHG vs. SFG.[17c] How exactly these effects come into play and why they differ for the two technical options, are interesting and crucial issues that have to be addressed in the future. Otherwise, quantitative conclusions about the electrochemical properties of the studied interfaces are meaningless if not completely misleading. For future studies, a comprehensive work that unifies the EDL picture independent of the technical approach would be a desirable goal.

All in all, nonlinear spectroscopy has provided new fundamental insights into mineral/water interfaces beyond the Gouy-Chapman description of electric double layers. To highlight only a few examples: It has been demonstrated for silica/water, that not only oppositely oriented sub-ensembles of water,[14g, 17b] but also hydrophobic species exist at this nominally hydrophilic surface.[30] Further, several species of surface hydroxyls with far-separated acidity have been identified.[14a] The screening properties of monovalent salts have been used to relate the NL response to interfacial ionic strengths and monitor interfacial dissolution kinetics.[14e, 69b] Another interesting and persistent question related to those studies is how the screening length of the surface potential and the surface charge are correlated. To approach this problem, one could think of using an electrode to apply an external potential. However, this electrode material would still have to fulfill the optical

constraints for SFG/SHG. Yet, first attempts in this direction have been made using graphene as electrode material deposited on a transparent substrate[70], but the chemical challenges that come along with this approach still require more engineering efforts in the future.

8.2 Potential consequences for geochemistry

8.2.1 Mineral dissolution

As discussed above, extensive studies employing nonlinear spectroscopic techniques have provided in-depth insights into the electrochemical and acid-base properties of various mineral/water interface. In nature, the contact between minerals and water occurs on a variety of timescales, making kinetic observations relevant for geochemistry. Yet only a few works have started to focus on the kinetic behavior of these interfaces, which ultimately determines the chemistry of these kinds of systems. In 2008, Geiger and coworkers reported an SHG work in EW geometry with p-in/all-out polarization, where they temporally resolved the pH titration of silica/water in the presence of 10-500 mM of salt.[69a] They found that the surface lags spatially and temporally the bulk pH, which, in case of the temporal delay, increased with increasing ionic strength and halide polarizability up to 4.5 h. Another study by the Bonn group highlighted the effect of flow on the silica/water interface, which seemed to reversibly alter the balance between the dissolution of silica and deprotonation of surface silanol groups.[5] Under neutral conditions and 10 mM background electrolytes, they observed a drop of the ssp SFG intensity of water upon flow, which recovered on a timescale of 30 minutes. They assigned this drop to a lowering in the effective surface charge resulting from a fast hydrolysis reaction of silica compared to slower deprotonation of the silanol groups under these conditions. As a follow-up of that work, Bonn and coworkers published a ssp SFG study that determined that the interfacial concentration of dissolved silica saturates in the millimolar range over a timescale of tens of hours. Moreover, the observed kinetics indicated that dissolution is an autocatalytic process.[69b] The notion of a shift in the dissolution equilibrium as a result of flow, seems like a generic property of mineral-water interfaces: as already mentioned in the CaF_2 section, also for this mineral flow can affect the interfacial equilibrium.[5] As, at acidic pH, fluoride dissolves more readily than calcium, the surface gets charged, and fluoride ions will be present in the near-surface region. Upon flow, the fluoride concentration in the near-surface region is modified, influencing the dissolution equilibrium.

8.2.2. Freezing at the mineral-water interface

Ice formation in the atmosphere occurs through heterogeneous nucleation, as homogeneous nucleation of ice cannot occur until temperatures below -40°C are reached. Mineral dust particles play a major role in heterogeneous ice nucleation [71], with different minerals displaying very different ice-nucleating capabilities. For instance, ice formation on the surface of feldspar particles was found to be remarkably efficient.[71] A combination of in situ scanning electron microscopy and molecular dynamic simulations revealed that nucleation occurs on specific defect sites of the feldspar surface.[72] The question presents itself what the underlying "rules" for efficient heterogeneous nucleation by minerals are. Therefore, in the past years, several groups[65d, 73] have studied changes in the SHG response and SFG spectrum upon freezing of water at mineral-water interfaces to understand the molecular-level details of this phase transition relevant for, e.g., atmospheric processes. In general, in agreement with an SHG study[65a] no change in the water structure is observed upon cooling as long as the water is liquid. Upon freezing different groups have reported different effects. In 2015, Leisner and coworkers performed temperature-dependent SHG measurements of the water/muscovite (001) interface.[65a] They observed, in contrast to the sapphire-water interface, a substantial change in the SHG response far above the freezing point of water, which they interpreted as preordering of interfacial water and facilitation of ice nucleation by the mica surface compared to the poor ice nucleator sapphire. A follow-up study discussed freezing mechanisms under varying conditions.[65b]

By comparing the freezing temperature with the amplitude of the ssp SFG signal in the liquid state, Bonn and coworkers[74] found that increasing the surface charge of the alumina (0001) surface through bulk pH variation, shifts freezing to a lower temperature and therefore suppresses ice nucleation. In turn, heterogeneous nucleation seemed to be most efficient at neutral alumina surface, i.e. around neutral pH, where the surface does not dictate the ordering of the interfacial water molecules. Moreover, a joint SFG, simulation, and nucleation-temperature study on the mica-water interface grafted with different positive ions, has shown that, also here, the ice nucleation ability depends on the water ordering at the interface [65e]. A reduced ordering of interfacial water was found to correlate with higher ice nucleation temperatures. This conclusion is in line with a temperature-dependent SFG study, using both ssp and ppp, from Dhinojwala and coworkers[65d] on the mica/water interface. They concluded that the orientation of water molecules next to the surface plays an important role in the structure of ice. SFG experiments (ssp) on the mica water interface with concentrations of sulfuric acid between 0.5 and 5 M showed a decreasing SFG signal

with increasing concentration of acid, interpreted as a reduced water ordering.[65c] The authors linked their results to the observation of higher acid concentrations resulting in poorer ice nucleation activity. They concluded that, apparently, structured water is needed for efficient heterogeneous ice nucleation. This seems to contradict the discussion above that reduced water ordering was associated with enhanced ice nucleation. However, at these high sulfate concentrations, sulfate may be absorbed at the surface and/or almost all water might be involved in the hydration of the sulfate ions resulting in a lack of free water.

8.3 Summary

In this review, we have summarized the extensive effort to study mineral/water interfaces with second-order nonlinear spectroscopy that started ~30 years ago and remains of increasing interest. By exploiting a large number of experimental degrees of freedom that SFG and SHG offer, this field has provided a variety of unique insights into these interfaces. For the three oxide interfaces silica, alumina, and titanium dioxide, the surface charge can be regulated by pH-dependent deprotonation and/or protonation. As the pzc for silica is around pH=2, the surface is negatively charged at near-neutral pH; for the other two surfaces, both positively and negatively charged surfaces are possible at typical pH, as the pzc is around 6. As the surface charge is pH-dependent, the second-order nonlinear signals vary with pH as well. Especially for silica, the research of the last years has focused on understanding what these spectroscopies measure. Consensus has been reached that for the charged silica surface, a major part of the signal in the hydrogen-bonded OH stretch region originates from bulk $\chi^{(3)}$ contributions. Increasing electrolyte concentrations reduces the signal strength mainly due to screening, but also ion-specific effects are observed. For charged titanium dioxide at low and high pH, the contribution of the bulk $\chi^{(3)}$-signal does not seem to dominate the response. For certain alumina interfaces also a response in the hydrogen-bonded region is observed, as well as a high-frequency mode close to 3700 cm^{-1} assigned to hydroxyl groups. For silica, in contrast, such a high-frequency mode has only been observed after special heat treatment of the surface. The CaF_2 surface is charged under low pH conditions due to the dissolution of fluoride. As a result, the water molecules orient to the interface resulting in a large second-order optical response. At high pH, fluoride exchanges with hydroxyl groups resulting in CaOH groups.

10.1002/anie.202003085

Although the discussed minerals have all a different chemical structure, many of the properties of the interfacial water structure seem dominated by the charge present at the mineral and much less by its chemical composition. For the interfacial chemistry, the detailed interfacial composition of the mineral is, of course, crucial.

We hope to have shown here that the research in the field of nonlinear optical studies of mineral-water surfaces has progressed to the point where we can start addressing geochemically and atmospherically relevant questions pertaining to interfacial chemistry under non-equilibrium conditions and, for instance, the mechanisms underlying heterogeneous nucleation of ice.

Acknowledgements

This work was funded by an ERC Starting Grant (Grant 336679). The authors thank Grazia Gonella for carefully reading the manuscript and Katharina Maisenbacher for expert help with the figures. We thank the MaxWater Initiative from the Max Planck Society for generous support

References

[1] F. Sebastiani, S. L. P. Wolf, B. Born, T. Q. Luong, H. Colfen, D. Gebauer, M. Havenith, *Angew. Chem.-Int. Edit.* **2017**, *56*, 490-495.

[2] M. J. Tang, D. J. Cziczo, V. H. Grassian, *Chem. Rev.* **2016**, *116*, 4205-4259.

[3] G. E. Brown, *Science* **2001**, *294*, 67-69.

[4] A. Putnis, *Science* **2014**, *343*, 1441-1442.

[5] D. Lis, E. H. G. Backus, J. Hunger, S. H. Parekh, M. Bonn, *Science* **2014**, *344*, 1138-1142.

[6] E. Brini, C. J. Fennell, M. Fernandez-Serra, B. Hribar-Lee, M. Luksic, K. A. Dill, *Chem. Rev.* **2017**, *117*, 12385-12414.

[7] L. Fumagalli, A. Esfandiar, R. Fabregas, S. Hu, P. Ares, A. Janardanan, Q. Yang, B. Radha, T. Taniguchi, K. Watanabe, G. Gomila, K. S. Novoselov, A. K. Geim, *Science* **2018**, *360*, 1339-+.

[8] aT. Fukuma, Y. Ueda, S. Yoshioka, H. Asakawa, *Phys. Rev. Lett.* **2010**, *104*, 4; bH. Imada, K. Kimura, H. Onishi, *Langmuir* **2013**, *29*, 10744-10751; cH. Songen, C. Marutschke, P. Spijker, E. Holmgren, I. Hermes, R. Bechstein, S. Klassen, J. Tracey, A. S. Foster, A. Kuhnle, *Langmuir* **2017**, *33*, 125-129; dK. Miyazawa, N. Kobayashi, M. Watkins, A. L. Shluger, K. Amano, T. Fukuma, *Nanoscale* **2016**, *8*, 7334-7342.

[9] aS. Yamamoto, H. Bluhm, K. Andersson, G. Ketteler, H. Ogasawara, M. Salmeron, A. Nilsson, *Journal of Physics-Condensed Matter* **2008**, *20*, 14; bS. Nemsak, A. Shavorskiy, O. Karslioglu, I. Zegkinoglou, A. Rattanachata, C. S. Conlon, A. Keqi, P. K. Greene, E. C. Burks, F. Salmassi, E. M. Gullikson, S. H. Yang, K. Liu, H. Bluhm, C. S. Fadley, *Nat. Commun.* **2014**, *5*, 7; cM. A. Brown, Z. Abbas, A. Kleibert, R. G. Green, A. Goel, S. May, T. M. Squires, *Phys. Rev. X* **2016**, *6*, 11007.

[10] A. Morita, *Theory of Sum Frequency Generation Spectroscopy*, Springer, Singapore **2018**.

[11] S. Roke, M. Bonn, A. V. Petukhov, *Phys. Rev. B* **2004**, *70*, 10.

[12] P. A. Covert, D. K. Hore, in *Annual Review of Physical Chemistry, Vol 67, Vol. 67* (Eds.: M. A. Johnson, T. J. Martinez), Annual Reviews, Palo Alto, **2016**, pp. 233-257.

[13] aX. Zhuang, P. B. Miranda, D. Kim, Y. R. Shen, *Phys. Rev. B* **1999**, *59*, 12632; bX. Wei, P. B. Miranda, C. Zhang, Y. R. Shen, *Phys. Rev. B* **2002**, *66*, 13.

[14] aS. Ong, X. Zhao, K. B. Eisenthal, *Chem. Phys. Lett.* **1992**, *191*, 327-335; bZ. Yang, Q. Li, K. C. Chou, *The Journal of Physical Chemistry C* **2009**, *113*, 8201-8205; cK. C. Jena, D. K. Hore, *J. Phys. Chem. C* **2009**, *113*, 15364-15372; dP. A. Covert, K. C. Jena, D. K. Hore, *J. Phys. Chem. Lett.* **2013**, *5*, 143-148; eJ. Schaefer, G. Gonella, M. Bonn, E. H. G. Backus, *Phys. Chem. Chem. Phys.* **2017**, *19*, 16875-16880; fK. A. Lovering, A. K. Bertram, K. C. Chou, *The Journal of Physical Chemistry C* **2016**, *120*, 18099-18104; gS.-h. Urashima, A. Myalitsin, S. Nihonyanagi, T. Tahara, *The Journal of Physical Chemistry Letters* **2018**, *9*, 4109-4114.

[15] M. D. Boamah, P. E. Ohno, F. M. Geiger, K. B. Eisenthal, *J. Chem. Phys* **2018**, *148*, 222808.

[16] aM. S. Azam, C. N. Weeraman, J. M. Gibbs-Davis, *J. Phys. Chem. Lett.* **2012**, *3*, 1269-1274; bM. S. Azam, C. N. Weeraman, J. M. Gibbs-Davis, *J. Phys. Chem. C* **2013**, *117*, 8840-8850; cM. S. Azam, A. Darlington, J. M. Gibbs-Davis, *J. Phys.-Condens. Mat.* **2014**, *26*, 244107; dA. M. Darlington, J. M. Gibbs-Davis, *J. Phys. Chem. C* **2015**, *119*, 16560-16567; eG. Gonella, C. Lütgebaucks, A. G. F. de Beer, S. Roke, *J. Phys. Chem. C* **2016**, *120*, 9165-9173.

[17] aS. Dewan, M. S. Yeganeh, E. Borguet, *J. Phys. Chem. Lett.* **2013**, *4*, 1977-1982; bA. Myalitsin, S. H. Urashima, S. Nihonyanagi, S. Yamaguchi, T. Tahara, *J. Phys. Chem. C* **2016**, *120*, 9357-9363; cA. M. Darlington, T. A. Jarisz, E. L. Dewalt-Kerian, S. Roy, S. Kim, M. S. Azam, D. K. Hore, J. M. Gibbs, *J. Phys. Chem. C* **2017**, *121*, 20229-20241; dE. L. DeWalt-Kerian, S. Kim, M. S. Azam, H. Zeng, Q. Liu, J. M. Gibbs, *The Journal of Physical Chemistry Letters* **2017**, *8*, 2855-2861.

[18] D. K. Hore, E. Tyrode, *J. Phys. Chem. C* **2019**, *123*, 16911-16920.

[19] aQ. Du, E. Freysz, Y. R. Shen, *Phys. Rev. Lett.* **1994**, *72*, 238; bV. Ostroverkhov, G. A. Waychunas, Y. R. Shen, *Chemical Physics Letters* **2004**, *386*, 144-148; cV. Ostroverkhov, G. A. Waychunas, Y. R. Shen, *Phys. Rev. Lett.* **2005**, *94*, 46102.

[20] K. C. Jena, P. A. Covert, D. K. Hore, *J. Phys. Chem. Lett.* **2011**, *2*, 1056-1061.

[21] Y.-C. Wen, S. Zha, X. Liu, S. Yang, P. Guo, G. Shi, H. Fang, Y. R. Shen, C. Tian, *Phys. Rev. Lett.* **2016**, *116*, 16101.

[22] A. Eftekhari-Bafrooei, E. Borguet, *J. Phys. Chem. Lett.* **2011**, *2*, 1353-1358.

[23] A. Tuladhar, S. Dewan, S. Pezzotti, F. Siro Brigiano, F. Creazzo, M. P. Gaigeot, E. Borguet, *J. Am. Chem. Soc.* **2020**, *142*, 6991-7000.

[24] M. D. Boamah, P. E. Ohno, E. Lozier, J. van Ardenne, F. M. Geiger, *The Journal of Physical Chemistry B* **2019**, *123*, 5848-5856.

[25] J. A. McGuire, Y. R. Shen, *Science* **2006**, *313*, 1945-1948.

[26] aA. Eftekhari-Bafrooei, E. Borguet, *J. Am. Chem. Soc.* **2009**, *131*, 12034-12035; bA. Eftekhari-Bafrooei, E. Borguet, *J. Am. Chem. Soc.* **2010**, *132*, 3756-3761.

[27] S. C. Flores, J. Kherb, N. Konelick, X. Chen, P. S. Cremer, *The Journal of Physical Chemistry C* **2012**, *116*, 5730-5734.

[28] B. Reh, M. Rashwan, E. L. DeWalt-Kerian, T. A. Jarisz, A. M. Darlington, D. K. Hore, J. M. Gibbs, *J. Phys. Chem. C* **2019**, *123*, 10991-11000.

[29] L. Dalstein, E. Potapova, E. Tyrode, *Phys. Chem. Chem. Phys.* **2017**, *19*, 10343-10349.

[30] J. D. Cyran, M. A. Donovan, D. Vollmer, F. Siro Brigiano, S. Pezzotti, D. R. Galimberti, M.-P. Gaigeot, M. Bonn, E. H. G. Backus, *Proceedings of the National Academy of Sciences* **2019**, *116*, 1520-1525.

[31] M. S. Azam, C. Y. Cai, J. M. Gibbs, E. Tyrode, D. K. Hore, *J. Am. Chem. Soc.* **2020**, *142*, 669-673.

[32] J. E. Bertie, Z. Lan, *Applied Spectroscopy* **1996**, *50*, 1047-1057.

[33] Q. Du, R. Superfine, E. Freysz, Y. R. Shen, *Phys. Rev. Lett.* **1993**, *70*, 2313.

[34] S. H. Chen, S. J. Singer, *J. Phys. Chem. B* **2019**, *123*, 6364-6384.

[35] E. L. DeWalt-Kerian, S. Kim, M. S. Azam, H. Zeng, Q. Liu, J. M. Gibbs, *The Journal of Physical Chemistry Letters* **2017**, *8*, 4793-4793.

[36] M. S. Yeganeh, S. M. Dougal, H. S. Pink, *Phys. Rev. Lett.* **1999**, *83*, 1179-1182.

[37] A. G. Stack, S. R. Higgins, C. M. Eggleston, *Geochimica et Cosmochimica Acta* **2001**, *65*, 3055-3063.

[38] J. P. Fitts, X. Shang, G. W. Flynn, T. F. Heinz, K. B. Eisenthal, *J. Phys. Chem. B* **2005**, *109*, 7981-7986.

[39] L. Zhang, C. Tian, G. A. Waychunas, Y. R. Shen, *J. Am. Chem. Soc.* **2008**, *130*, 7686-7694.

[40] A. Tuladhar, S. M. Piontek, E. Borguet, *J. Phys. Chem. C* **2017**, *121*, 5168-5177.

[41] M. Florsheimer, K. Kruse, R. Polly, A. Abdelmonem, B. Schimmelpfennig, R. Klenze, T. Fanghanel, *Langmuir* **2008**, *24*, 13434-13439.

[42] B. Braunschweig, S. Eissner, W. Daum, *J. Phys. Chem. C* **2008**, *112*, 1751-1754.

[43] J. H. Sung, L. N. Zhang, C. S. Tian, Y. R. Shen, G. A. Waychunas, *J. Phys. Chem. C* **2011**, *115*, 13887-13893.

[44] J. Sung, Y. R. Shen, G. A. Waychunas, *Journal of Physics-Condensed Matter* **2012**, *24*.

[45] A. Boulesbaa, E. Borguet, *J. Phys. Chem. Lett.* **2014**, *5*, 528-533.

[46] A. Tuladhar, S. Dewan, J. D. Kubicki, E. Borguet, *J. Phys. Chem. C* **2016**, *120*, 16153-16161.

[47] Y. J. Tong, J. Wirth, H. Kirsch, M. Wolf, P. Saalfrank, R. K. Campen, *J. Chem. Phys.* **2015**, *142*, 12.

[48] A. Tuladhar, S. M. Piontek, L. Frazer, E. Borguet, *J. Phys. Chem. C* **2018**, *122*, 12819-12830.

[49] S. M. Piontek, A. Tuladhar, T. Marshall, E. Borguet, *J. Phys. Chem. C* **2019**, *123*, 18315-18324.

[50] J. Lutzenkirchen, G. V. Franks, M. Plaschke, R. Zimmermann, F. Heberling, A. Abdelmonem, G. K. Darbha, D. Schild, A. Filby, P. Eng, J. G. Catalano, J. Rosenqvist, T. Preocanin, T. Aytug, D. Zhang, Y. Gan, B. Braunschweig, *Adv. Colloid Interface Sci.* **2018**, *251*, 1-25.

[51] K. A. Becraft, G. L. Richmond, *Langmuir* **2001**, *17*, 7721-7724.

[52] R. Khatib, E. H. G. Backus, M. Bonn, M. J. Perez-Haro, M. P. Gaigeot, M. Sulpizi, *Scientific Reports* **2016**, *6*, 1-10.

[53] N. Kobayashi, S. Itakura, H. Asakawa, T. Fukuma, *J. Phys. Chem. C* **2013**, *117*, 24388-24396.

[54] D. Lesnicki, Z. Zhang, M. Bonn, M. Sulpizi, E. H. G. Backus, *submitted* **2020**.

[55] A. Boulesbaa, E. Borguet, *J. Phys. Chem. Lett.* **2016**, *7*, 5080-5085.

[56] A. N. Bordenyuk, A. V. Benderskii, *J. Chem. Phys.* **2005**, *122*, 134713.

[57] A. J. Hopkins, S. Schrödle, G. L. Richmond, *Langmuir* **2010**, *26*, 10784-10790.

[58] J. Lutzenkirchen, T. Scharnweber, T. Ho, A. Striolo, M. Sulpizi, A. Abdelmonem, *J. Colloid Interface Sci.* **2018**, *529*, 294-305.

[59] S. Kataoka, M. C. Gurau, F. Albertorio, M. A. Holden, S. M. Lim, R. D. Yang, P. S. Cremer, *Langmuir* **2004**, *20*, 1662-1666.

[60] K. Uosaki, T. Yano, S. Nihonyanagi, *J. Phys. Chem. B* **2004**, *108*, 19086-19088.

[61] S. Hosseinpour, F. Tang, F. Wang, R. A. Livingstone, S. J. Schlegel, T. Ohto, M. Bonn, Y. Nagata, E. H. G. Backus, *J. Phys. Chem. Lett.* **2017**, *8*, 2195-2199.

[62] S. J. Schlegel, S. Hosseinpour, M. Gebhard, A. Devi, M. Bonn, E. H. G. Backus, *Physical Chemistry Chemical Physics* **2019**, *21*, 8956-8964.

[63] P. B. Miranda, L. Xu, Y. R. Shen, M. Salmeron, *Phys. Rev. Lett.* **1998**, *81*, 5876.

[64] A. Tuladhar, Z. A. Chase, M. D. Baer, B. A. Legg, J. Tao, S. Zhang, A. D. Winkelman, Z. Wang, C. J. Mundy, J. J. De Yoreo, H. F. Wang, *J. Am. Chem. Soc.* **2019**, *141*, 2135-2142.

[65] aA. Abdelmonem, J. Lützenkirchen, T. Leisner, *Atmospheric Measurement Techniques* **2015**, *8*, 3519-3526; bA. Abdelmonem, *Atmos. Chem. Phys.* **2017**, *17*, 10733-10741; cZ. Yang, A. K. Bertram, K. C. Chou, *J. Phys. Chem. Lett.* **2011**, *2*, 1232-1236; dE. Anim-Danso, Y. Zhang, A. Dhinojwala, *J. Phys. Chem. C* **2016**, *120*, 3741-3748; eS. Jin, Y. Liu, M. Deiseroth, J. Liu, E. H. G. Backus, H. Li, H. Xue, L. Zhao, X. C. Zeng, M. Bonn, J. Wang, *submitted* **2020**.

[66] aC. S. Tian, Y. R. Shen, *Chemical Physics Letters* **2009**, *470*, 1-6; bC.-S. Tian, Y. R. Shen, *J. Am. Chem. Soc.* **2009**, *131*, 2790-2791; cS. Nihonyanagi, T. Ishiyama, T.-K. Lee, S. Yamaguchi, M. Bonn, A. Morita, T. Tahara, *J. Am. Chem. Soc.* **2011**, *133*, 16875-16880.

[67] aS. Nihonyanagi, R. Kusaka, K. I. Inoue, A. Adhikari, S. Yamaguchi, T. Tahara, *J. Chem. Phys.* **2015**, *143*; bS. Sun, R. Liang, X. Xu, H. Zhu, Y. R. Shen, C. Tian, *J. Chem. Phys.* **2016**, *144*.

[68] aV. Mizrahi, J. E. Sipe, *J. Opt. Soc. Am. B* **1988**, *5*, 660-667; bR.-r. Feng, Y. Guo, R. Lü, L. Velarde, H.-f. Wang, *J. Phys. Chem. A* **2011**, *115*, 6015-6027; cE. H. G. Backus, N. Garcia-Araez, M. Bonn, H. J. Bakker, *J. Phys. Chem. C* **2012**, *116*, 23351.

[69] aJ. M. Gibbs-Davis, J. J. Kruk, C. T. Konek, K. A. Scheidt, F. M. Geiger, *J. Am. Chem. Soc.* **2008**, *130*, 15444-15447; bJ. Schaefer, E. H. G. Backus, M. Bonn, *Nat. Commun.* **2018**, *9*, 3316.

[70] aL. B. Dreier, Z. Liu, A. Narita, M. J. van Zadel, K. Mullen, K. J. Tielrooij, E. H. G. Backus, M. Bonn, *J. Phys. Chem. C* **2019**, *123*, 24031-24038; bY. W. Zhang, H. B. de Aguiar, J. T. Hynes, D. Laage, *J. Phys. Chem. Lett.* **2020**, *11*, 624-631.

[71] J. Atkinson, B. Murray, M. Woodhouse, T. Whale, K. Baustian, K. Carslaw, S. Dobbie, D. O'Sullivan, *Nature* **2013**, *498*, 355-358.

[72] A. Kiselev, F. Bachmann, P. Pedevilla, S. J. Cox, A. Michaelides, D. Gerthsen, T. Leisner, *Science* **2017**, *355*, 367-371.

[73] aE. Anim-Danso, Y. Zhang, A. Alizadeh, A. Dhinojwala, *J. Am. Chem. Soc.* **2013**, *135*, 2734-2740; bE. Anim-Danso, Y. Zhang, A. Dhinojwala, *J. Am. Chem. Soc.* **2013**, *135*, 8496-8499; cK. A. Lovering, A. K. Bertram, K. C. Chou, *J. Phys. Chem. Lett.* **2017**, *8*, 871-875; dA. Abdelmonem, S. Ratnayake, J. D. Toner, J. Lutzenkirchen, *Atmos. Chem. Phys.* **2020**, *20*, 1075-1087.

[74] A. Abdelmonem, E. H. G. Backus, N. Hoffmann, M. A. Sánchez, J. D. Cyran, A. Kiselev, M. Bonn, *Atmos. Chem. Phys.* **2017**, *17*, 7827-7837.

10.1002/anie.202003085

Biographical sketches

Ellen Backus

Ellen Backus is professor for physical chemistry at the University of Vienna and a group leader at the Max Planck Institute for polymer research in Mainz. Her research focusses on the molecular structure and (ultrafast) dynamics of various aqueous interfaces by using surface-specific vibrational spectroscopy. She obtained her PhD in 2005 at the Leiden University. After postdoctoral stays at the University of Zurich and at AMOLF in Amsterdam, she has worked since 2012 in Mainz and started in 2018 in Vienna.

Jan Schaefer

Jan Schäfer received his PhD in 2019 from the University of Mainz for his work at the Max Planck Institute for Polymer Research. His studies focussed on Sum Frequency Generation spectroscopy experiments on non-equilibrium aqueous interfacial systems. Before, he received a Master degree at Ruhr University of Bochum for his spectroscopic studies of water clusters with organic radicals in ultracold Helium nanodroplets. Currently, he is affiliated with Coherent Shared Services B.V. Europe.

10.1002/anie.202003085

Mischa Bonn

Mischa Bonn serves as Max Planck Director at the Institute for Polymer Research in Mainz, Germany, where he heads the Department of Molecular Spectroscopy, following appointments at the FOM-Institute for Atomic and Molecular Physics in Amsterdam, and Leiden University. The central theme of Mischa's research is the characterization and control of the structure and dynamics of molecules, specifically at interfaces. Water is Mischa's favorite molecule.